$\mathcal{A} \cdot 8\,7\!6$ APR 2   1976

HIGH PERFORMANCE N_2O_4/AMINE ELEMENTS
FINAL REPORT

NASA CR
147555

March 1976

by

A. Y. Falk

Prepared for

National Aeronautics and Space Administration
Lyndon B. Johnson Space Center

ROCKWELL INTERNATIONAL/ROCKETDYNE DIVISION
6633 Canoga Avenue
Canoga Park, California
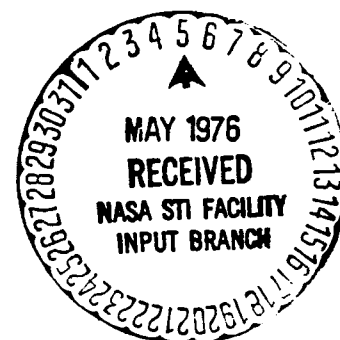
HIGH PERFORMANCE N_2O_4/AMINE ELEMENTS
FINAL REPORT

March 1976

Prepared by

A. Y. Falk

Approved by

[signature]

W. H. Nurick
Program Manager
Combustion Programs

Prepared for
National Aeronautics and Space Administration
Lyndon B. Johnson Space Center

ROCKWELL INTERNATIONAL/ROCKETDYNE DIVISION
6633 Canoga Avenue
Canoga Park, California

FOREWORD

This report was prepared for the NASA Lyndon B. Johnson Space Center, Houston, Texas by the Advanced Programs Department of Rocketdyne Division, Rockwell International. The study was conducted in accordance with Contract NAS9-14126, Rocketdyne G.O. 09640. Mr. M. F. Lausten of the Lyndon B. Johnson Space Center served as the NASA Technical Manager. The Rocketdyne Program Manager was Mr. W. H. Nurick.

The work conducted on this contract is summarized in Rocketdyne Report R-9847-2.

ABSTRACT

An analytical and experimental investigation was conducted to develop an understanding of the mechanisms that cause reactive stream separation, commonly called "blowapart," for hypergolic propellants. The investigation was limited to the N_2O_4/MMH propellant combination and to a range of engine-operating conditions applicable to the Space Tug and Space Shuttle attitude control and orbital maneuvering engines. Primary test variables were: chamber pressure (1 to 20 atm), fuel injection temperature (283 to 400°K)m and propellant injection velocity (9 to 50 m/s). The injector configuration studied was the unlike doublet. The reactive stream separation experiments were conducted using special combustors designed to permit photography of the near-injector spray combustion flow field. Analysis of color motion pictures provided the means of determining the occurrence of reactive stream separation.

Through a basic understanding of the governing mechanisms, meaningful design criteria were established which defined regions of operation that are free from reactive stream separation for N_2O_4/MMH propellants.

CONTENTS

ILLUSTRATIONS

TABLES

1.0 SUMMARY

The objective of this program was to develop an understanding of the mechanisms that cause reactive stream separation, commonly called "blowapart", for hypergolic propellants. Analytical and experimental investigations were conducted to accomplish this objective. The study was limited to the N_2O_4/MMH propellant combination and to a range of engine operating conditions applicable to the Space Tug and Space Shuttle attitude control and orbital maneuvering engines.

Primary test variables were: chamber pressure (1 to 20 atm; 13.7 to 300 psia), fuel injection temperature (283 to 400°K; 50 to 260°F), and propellant injection velocity (9 to 50 m/s; 30 to 160 ft/sec). Nominal mixture ratio for all tests was ~1.7, the equal volume value for the N_2O_4/MMH propellant combination. The injector configuration studied was the unlike doublet. The reactive stream separation experiments were conducted using special combustors designed to permit photography of the near-injector spray combustion flow field. Analysis of the color motion pictures provided the means of determining the occurrence of reactive stream separation.

Two types of reactive stream separation, with different driving mechanisms, were observed during the conduct of the program. One of them, termed penetration, occurred at high injection velocities and/or chamber pressures with ambient or moderately heated (fuel) propellants. The other phenomena, termed separation, occurred at elevated fuel temperatures. Through a basic understanding of the governing mechanisms, design criteria were established which defined regions of operation that are free from reactive stream separation for N_2O_4/MMH propellants.

To prevent penetration, the design criteria established was that the fuel stream Weber number be less than 14. That is

$$\text{Weber Number} = \frac{\rho_g v_f^2 d_f}{\sigma_f g_c} < 14$$

To prevent separation, which can occur with heated propellants, the injector design should be based on the following criteria

$$\frac{x_c}{L_c} = \frac{1}{\Delta E A} e^{\Delta E / R_g T_o} \left[\frac{v_f T_o^3 C_p \rho_\ell R_g^2}{C_4 P \Delta H} \right]$$

where

$$\frac{x_c}{L_c} < 1 \quad \text{gives separation}$$

$$\frac{x_c}{L_c} > 1 \quad \text{gives mixing}$$

$$\frac{x_c}{L_c} = 1 \quad \text{is the boundary between separation and mixing}$$

The value of all quantities require to calculate x_c/L_c are known. Evaluation of the constants C_4, A, and ΔE were determined by correlation of the experimental data. The design criteria were based on the experimental data of this contract (NAS9-14126) and a related effort conducted by Aerojet (NAS9-14186).

2.0 INTRODUCTION

2.1 OBJECTIVE

The objective of this program was to develop an understanding of the mechanisms that cause reactive stream separation (RSS), commonly called "blowapart", for hypergolic propellants. Through a basic understanding of the governing mechanisms, design criteria were to be established which would allow the design of stable high performing injectors that are free from RSS and "pops" (cyclic blowapart).

2.2 BACKGROUND

Hypergolic earth-storable propellants such as N_2O_4/amine-type fuels are prime candidates for use on the Space Shuttle attitude control and orbital maneuvering engines (OME) as well as for Space Tug applications. These types of hypergolic propellants, being highly reactive, can experience reactive stream separation and/or cyclic blowapart (popping) under some conditions. The former is a quasi steady-state phenomenon that, for impinging jet injector designs, turns the propellant streams away from each other so that intra-element propellant mixing is impaired. This causes poor overall propellant mixing uniformity and thereby, results in lowered combustion efficiency. Cyclic blowapart (or popping) is caused by small explosions that occur in the spray mixing region. These explosions or "pops" can sustain and/or drive acoustic instabilities as well as result in cyclic disruption of the mixing process which can lower the overall time averaged combustion efficiency. Because of the extremely high combustion efficiencies and reliability required for current applications, it is imperative that the cyclic blowapart and reactive stream separation phenomenon be understood and their undesirable effects be minimized.

Over the past 15 years, numerous studies have been conducted in efforts to identify the reactive stream separation and/or popping operating limits

as well as to develop injector design criteria for their avoidance.
Examples of some of these studies are those of Refs. 1 through 24.
Both RSS and popping have been experimentally observed and several
physical models postulated. Unfortunately, none of the existing models
can to date account for all of the experimentally determined RSS or
popping. Existing models give satisfactory correlation of only selected
sets of available experimental data. This defect is due to a lack of a
clear understanding of the physical/chemical processes controlling the
various phenomena as well as the interaction of competing mechanisms.
Meaningful rocket engine design criteria that will ensure blowapart-free
operation can result only from determination of: (1) the explosion and
separation mechanisms, and (2) their relationship to engine operating
conditions and injector design specifications. A survey of existing
information provided the background for this study.

2.3 SCOPE

This investigation was limited to the N_2O_4/MMH propellant combination and
to a range of engine operating conditions applicable to the Space Tug and
Space Shuttle attitude control and orbital maneuvering engines as defined in
Table 2-1. The injector configurations studies were single-element unlike
doublets.

TABLE 2-1. RANGE OF COMBUSTOR OPERATING CONDITIONS FOR INVESTIGATION

Chamber pressure	4 to 20 atm	(60-300 psia)
Mixture ratio	1.6 to 2.2	
Fuel temperature	277 to 394°K	(40 to 250°F)
Oxidizer temperature	277 to 339°K	(40 to 150°F)
Minimum orifice diameter	0.0508 cm	(0.020-inch)
Maximum orifice diameter	0.1016 cm	(0.040-inch)
Injection ΔP	0.7 to 17 atm	(10 to 250 psi)

Hot-fire testing and analyses were conducted to establish meaningful
design criteria for stable high performing injectors that are free
from pops and RSS.

3.0 TECHNICAL APPROACH

To accomplish the objectives of this program, the overall program was divided into four separate tasks.

Task I	-	Review of Existing Models and Experimental Data
Task II	-	Program Plan Preparation
Task III	-	Definition of Governing Mechanisms
Task IV	-	Unlike-doublet Steady-state Reactive Stream Separation

The objective of the Task I effort was to provide an up-to-date knowledge of pertinent theoretical models and experimental data for guidance in subsequent tasks. Pertinent models and data were critically reviewed. The results of this effort were summarized in a semi-formal data dump report (Rocketdyne Report R-9594; Ref. 25).

The objective of the Task II effort was to formulize, in detail, the scope of investigation, the experimental and analytical approaches to be employed in achieving the program goals, and the hardware and the number and type of experiments required. A program plan describing the above was prepared, based on results of the Task I effort, and it was reviewed with and approved by the NASA technical monitor.

The objective of Task III was to define the governing mechanisms and parameters causing reactive stream separation for inclusion in appropriate physical models of the experimental results. Experiments were conducted (Section 5.0) and the results analyzed (Section 6.0) to accomplish this objective.

The objective of the Task IV effort was to further establish the operating limits for reactive stream separation for the unlike-doublet element. As is noted in Section 6.0 of this report, this objective was accomplished.

This report and a companion report (R-9847-2) present the results of the program and, thereby, conclude the contractual data.

4.0 EXPERIMENTAL SYSTEM

The test facility, experimental hardware, and photographic technique employed are described herein.

4.1 TEST FACILITY

The reactive stream separation experiments were performed on test stand Victor in the Propulsion Research Area (PRA) of Rocketdyne's Santa Susana Field Laboratory (SSFL) using special combustors designed to permit photography of the near-injector spray combustion flow field.

4.1.1 Test Stand

Victor test stand, as used in the hot firing experiments, is shown schematically in Fig. 4-1. The oxidizer (N_2O_4) was fed from a high pressure 750-liter (200-gallon) supply tank to the Victor stand pre-valve, through a 40-micron filter, a thermal-conditioning system (water bath) for tests with other than ambient temperature oxidizer, a sharp-edge orifice for flow measurement, the engine shutoff valve, and into the injector. For ambient temperature tests, the thermal conditioning system was by-passed. The fuel (MMH) was fed from a 190-liter (50-gallon) run tank, through a filter, a water-jacketed line, a sharp-edge orifice or flowmeter, the engine shut-off valve, and into the injector. The liquid propellants were forced from their respective tanks by regulated GN_2 pressure from a 194-atm (2850 psig) supply bottle.

Conditioning of the propellants to other than ambient temperature was accomplished by heat exchange with hot or cold water. For heating, hot water (electrically heated) was used in preference to direct electrical heating of the propellants because it insured that surfaces in direct contact with the propellants could not exceed safe temperatures defined by thermal stability or corrosive tendencies. For tests in which propellant injection
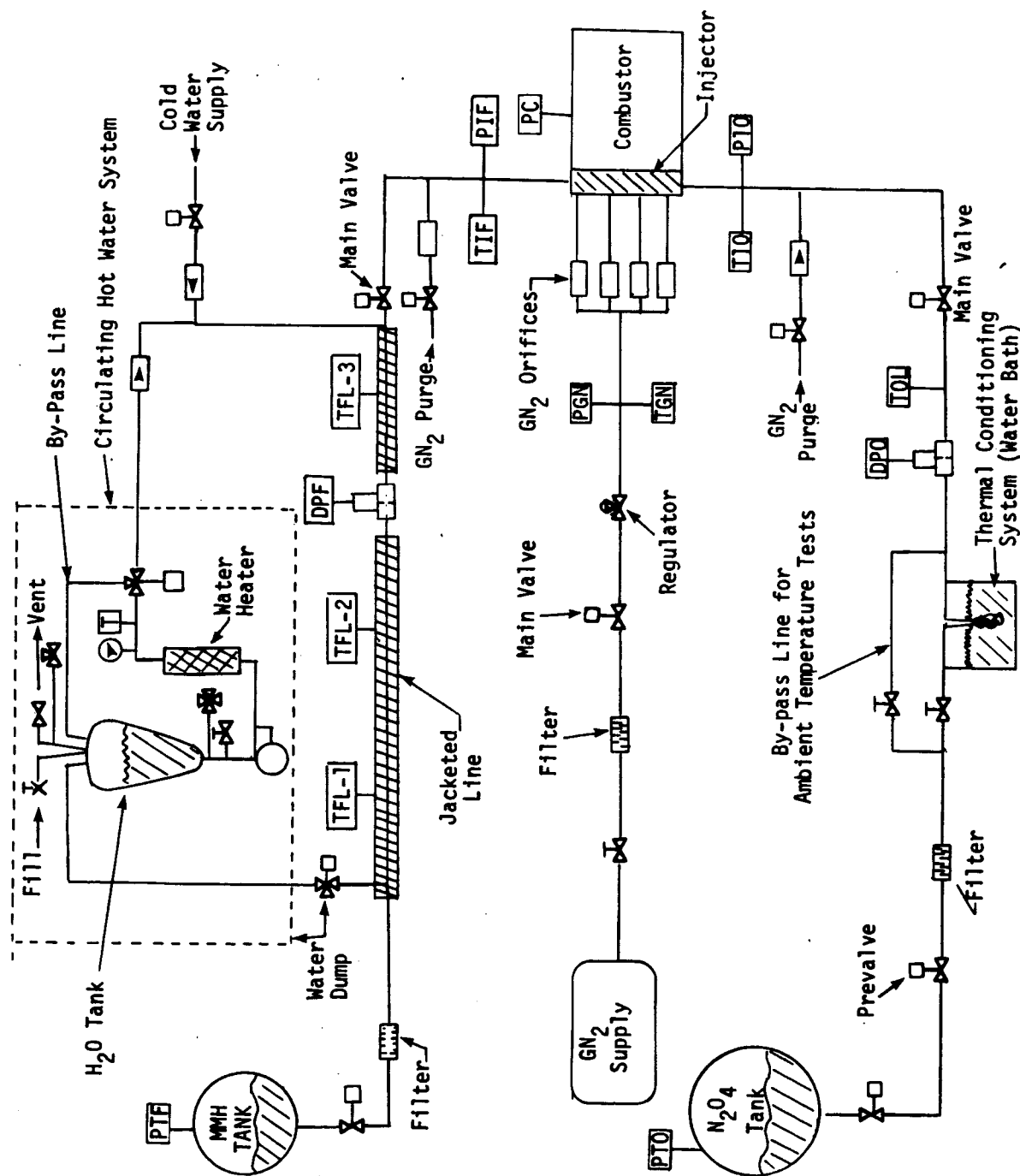
Figure 4-1. Schematic of Test Stand Used for Hot-Firing Experiments (Victor Stand PRA)

temperatures below ambient temperature were required, conditioning
was accomplished using cold (ice) water. The N_2O_4 was conditioned
(277 to 339°K; 40 to 150°F) by passage through two 15.24-m (50 ft.)
coils of 1.27-cm (½-inch) diameter tubing immersed in a water bath.
The fuel was conditioned (277 to 394°K; 40 to 250°F) by passing cold
or hot water through the jacket on the run line. Heating was accom-
plished with a closed-loop circulating hot water system. Cooling was
accomplished by means of flushing cold water through the line jacket.

To permit variation of chamber pressure at fixed propellant injection
conditions (i.e., flowrate, injection velocity, etc.), a regulated
gaseous nitrogen (GN_2) combustion chamber bleed system was employed in
conjunction with a fixed combustor throat area. Regulation of the GN_2
flowrate in conjunction with the propellant flowrates made it possible
to vary chamber pressure at fixed injection conditions. The nitrogen
bleed was regulated from a 194-atm (2850 psig) supply bottle to ap-
proximately twice the planned operating chamber pressure and then passed
through sonic orifices in four 2.54 cm (1-inch) diameter lines to the
inlet GN_2 manifold ports in the injector. This GN_2 bleed provided most
of the desired combustion chamber pressure.

4.1.2 Instrumentation

Pressure and temperature measurements made to define and/or control pro-
pellant injection (flowrate and temperature) and combustor operating
conditions are presented in Table 4-1. Locations of the various measure-
ments are noted in Fig.4-1 in which the measurement nomenclature corresponds
to that defined in Table 4-1.

Pressures and pressure differentials (ΔP) were measured with calibrated
Tabor strain gage transducers. Temperatures were measured with iron/
constantan thermocouple probes. Chamber pressure and fuel and oxidizer
manifold pressure oscillations were measured in some of the early testing
using Kistler transducers. However, meaningful data with regard to reactive
stream separation was not obtained from these measurements so they were
discontinued.

TABLE 4-1. INSTRUMENTATION LIST FOR REACTIVE STREAM SEPARATION EXPERIMENTS

PARAMETER	SYMBOL (Fig. 4-1)
Chamber pressure	PC
Oxidizer tank pressure	PTO
*Oxidizer line orifice ΔP	DPO
Oxidizer line temperature	TLO
Oxidizer injection temperature	TIO
Oxidizer injection pressure	PIO
Fuel tank pressure	PTF
Fuel line temperature #1	TFL-1
Fuel line temperature #2	TFL-2
Fuel line temperature #3	TFL-3
*Fuel line orifice ΔP	DPF
Fuel injection temperature	TIF
Fuel injection pressure	PIF
GN_2 line pressure	PGN
GN_2 line temperature	TGN
Fuel system hot water temperature	T

*Orifice ΔP from calibrated orifices was used to calculate propellant flowrate. At the higher flowrates a turbine flowmeter was employed in the fuel system.

4.2 HARDWARE

The experimental hardware consisted of two basic components: (1) an injector assembly, and (2) a combustion chamber assembly. The injector assembly contained two separately manifolded unlike-doublet elements. Two different combustion chamber assemblies, both of which permitted pictures to be taken of the doublet spray pattern, were employed. These components are described below.

4.2.1 Combustion Chamber

Two combustion chamber assemblies of different design were employed. One of these was a high contraction ratio ($\varepsilon_c \cong 77$) tapered chamber. The other was a low contraction ratio ($\varepsilon_c \cong 12$) cylindrical chamber. Schematics of the tapered and cylindrical chambers are presented as Figs. 4-2 and 4-3, respectively. Both chambers employed the same basic injector assembly and had the same throat area (~ 5 cm^2; 0.77 in.^{2}). Minor modification of the injector assembly, as is noted in Section 4.2.1.2, was necessary to adapt the injector to the low contraction ratio chamber after its initial use in the high contraction rate chamber.

4.2.1.1 High Contraction Ratio Tapered Chamber. A photograph of the major combustor components for the high contraction ratio tapered chamber assembly is shown in Fig. 4-4 (Rocketdyne Drawing No. AP74-601). The design of this assembly was based upon hardware previously employed at Rocketdyne (Ref. 21) and incorporated the following features:

1. Two viewing windows located diametrically opposite each other so as to permit pictures to be taken of the doublet spray pattern.

2. Capability to vary chamber pressure independent of propellant injection rate by variation of a GN$_2$ base bleed flowrate.

Figure 4-2. Schematic Illustration of High Contraction Ratio Tapered Combustor Assembly
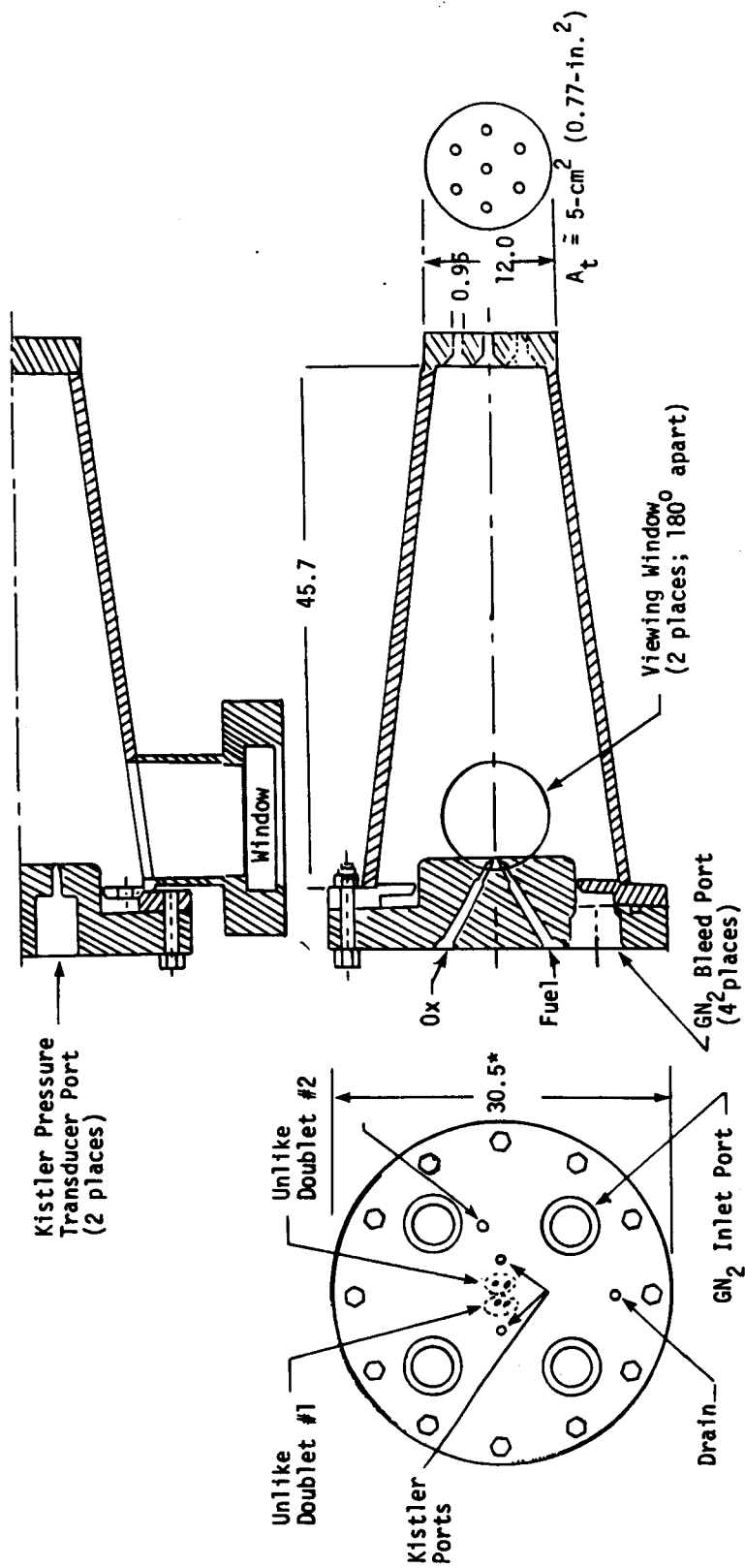
*Dimensions are in centimeters

4-6
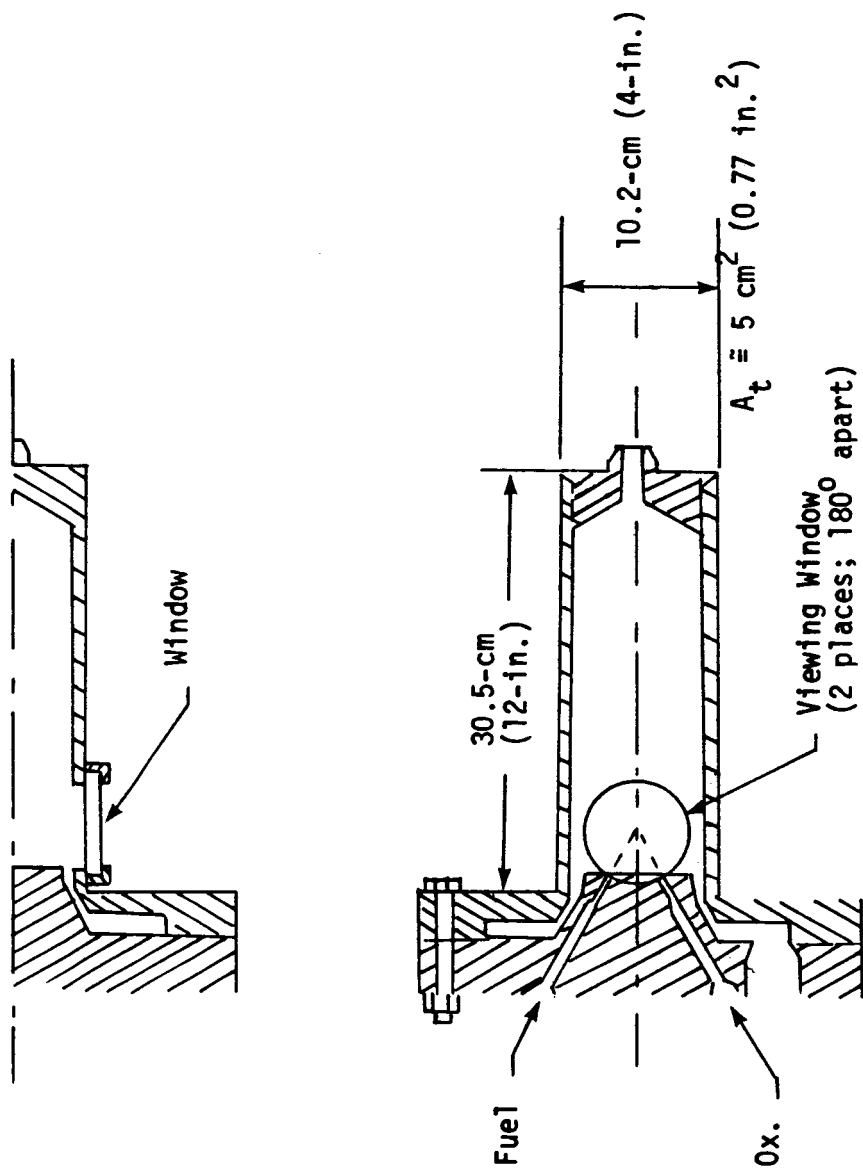
Figure 4-3. Schematic Illustration of Low Contraction Ratio Cylindrical Combustor Assembly
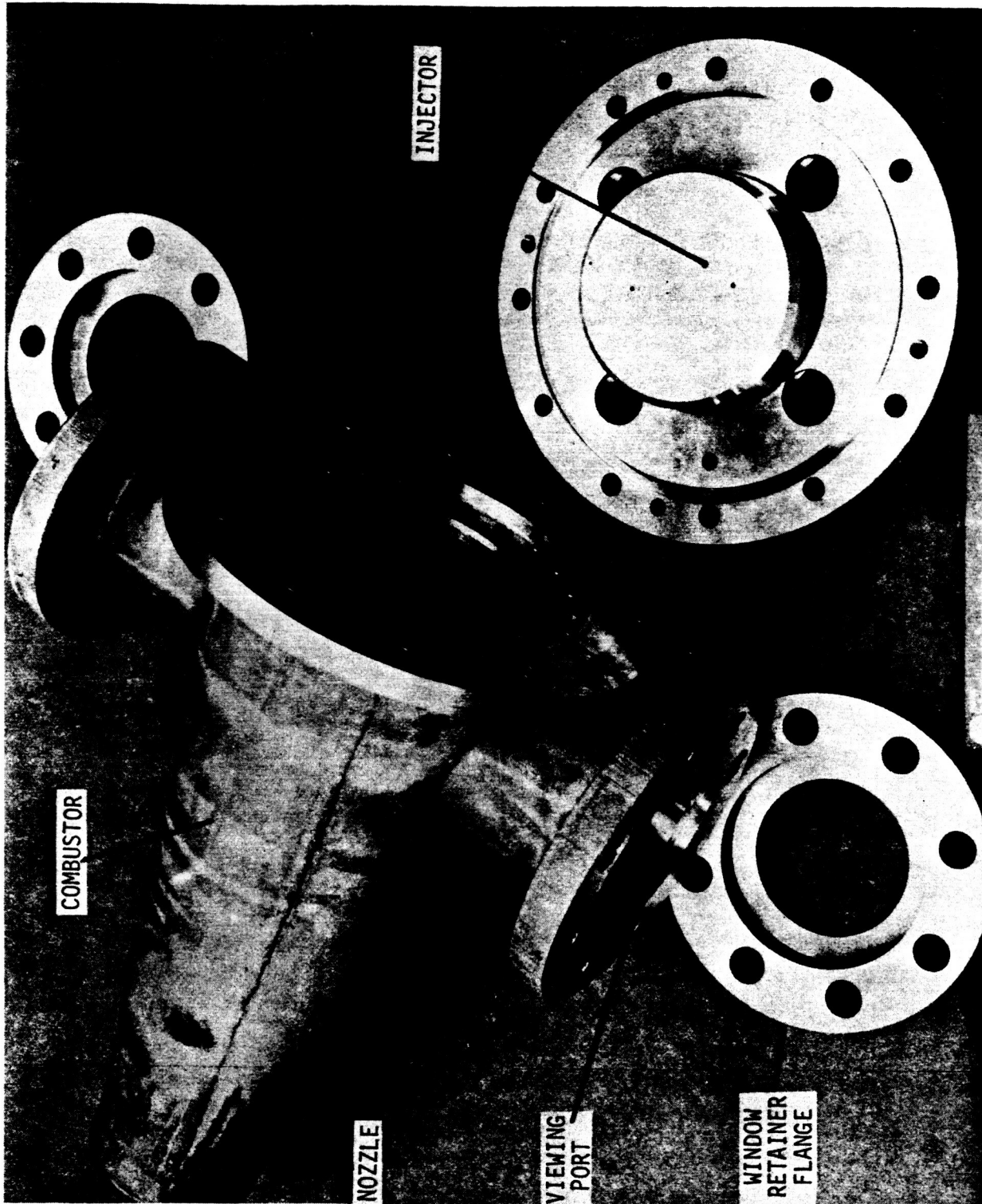
5AA34-10/29/74-S1D

Figure 4-4. Photograph of High Contraction Ratio Tapered Chamber Assembly

3. Use of the GN_2 bleed to protect both the windows and combustor walls from hot combustion gases, permitting repeated tests of any desired duration in an economical and otherwise uncooled system.

4. The GN_2 bleed (which had flowrates from 10 to 30 times the injected propellant flows) was expected to sweep away unreacted spray or recirculating N_2O_4 vapors which had previously inter-ferred with photographic studies in high contraction ratio chambers.

As is noted in Section 5.0 (Experimental Results), this latter feature did not work well in the high contraction ratio chamber. Consequently, a low contraction ratio cylindrical chamber was designed and employed for the latter portion of the hot-fire testing.

The initial (high contraction ratio) chamber was tapered over a chamber length of 46-cm (18-inches) from an inside diameter of 22.1 cm (8.7-inch) at the injector end to a diameter of 10.2-cm (4-inch) at the sonic orifice end plate. The convergence of the chamber walls was intended to provide a favorable pressure gradient which, together with a distributed system of tapering nozzles in the sonic orifice end plate, was expected to mini-mize gross recirculation patterns within the chamber. Because a high ratio of GN_2 bleed to combustor gas minimizes the heat transfer to the chamber walls, the combustor was rolled from 0.952-cm (3/8-inch) mild steel plate rather than more expensive copper or stainless steel ordin-arily used in heat sink chambers.

The windows in the tapered chamber were 12.7-cm (5-inch) diameter by 2.54-cm (1-inch) thick Pyrex discs. They were held in place by bolted flanges in bosses fabricated from standard 10.16-cm (4-inch) Schedule 40 pipe with an inside diameter of 10.3-cm (4.06-inch; see Fig.4-4). Cor-responding openings were provided in the flanges while a circular open-ing of 9.65-cm (3.8-inches) where the window cavity intersects the main chamber wall defines the backlighted field of vision from the windows.

Soft JM gaskets were used around the windows to provide both a pressure
seal and a cushion during the initial bolt tightening and subsequent
thermal expansions. The windows were located ~20-cm (8-inches) from the
vertical combustion chamber centerline and provided a field of vision
from the injector face ~7.6-cm (3-inches) downstream of the element im-
pingement points.

The GN_2 bleed was fed primarily through a system of 24 ports, each
1.27-cm (0.50-inch) in diameter, located near the outer periphery of
the chamber end flange as shown in Fig. 4-5. A secondary bleed was also
provided through the annular gap between the inner diameter of the
chamber end flange and the extension of the injector into the chamber
(see Fig.4-2). Both bleed inlet systems were fed from a ring manifold
in the injector flange which was in turn fed through four standard 3.81-cm
(1.5-inch) AN ports in the injector (Fig. 4-2).

Chamber pressure during the hot firing experiments resulted from the
choking effect of seven sonic orifices located in the chamber end plate
as shown in Fig. 4-2. Each orifice was 0.9525-cm (0.375-inch) in
diameter with a short 45° chamfered entrance. The distributed throat
was provided in an attempt to reduce recirculation in the high contraction
ratio chamber.

4.2.1.2 <u>Low Contraction Ratio Cylindrical Chamber</u>. The high contraction
ratio tapered chamber was employed for the first 199 tests. Satisfactory
movies of the impinging streams were not obtained for many of these tests
because of gross recirculation which occurred in the combustor. $N_2O_4/$
combustion products obstructed the view of the impinging streams for many
of these tests. To overcome this difficulty, the chamber (combustor) design
was revised to suppress recirculation and, thereby, permit better photographs
to be taken of the impinging streams. The chamber volume (diameter and
length) was reduced and the viewing windows were mounted essentially flush
rather than recessed (see Figs. 4-2 and 4-3). This design proved to be better

GN$_2$ Bleed Port
(24 Places)

Chamber Nozzle
Throat Orifice
(7 Places)

Viewing
Port Boss
(2 Places)
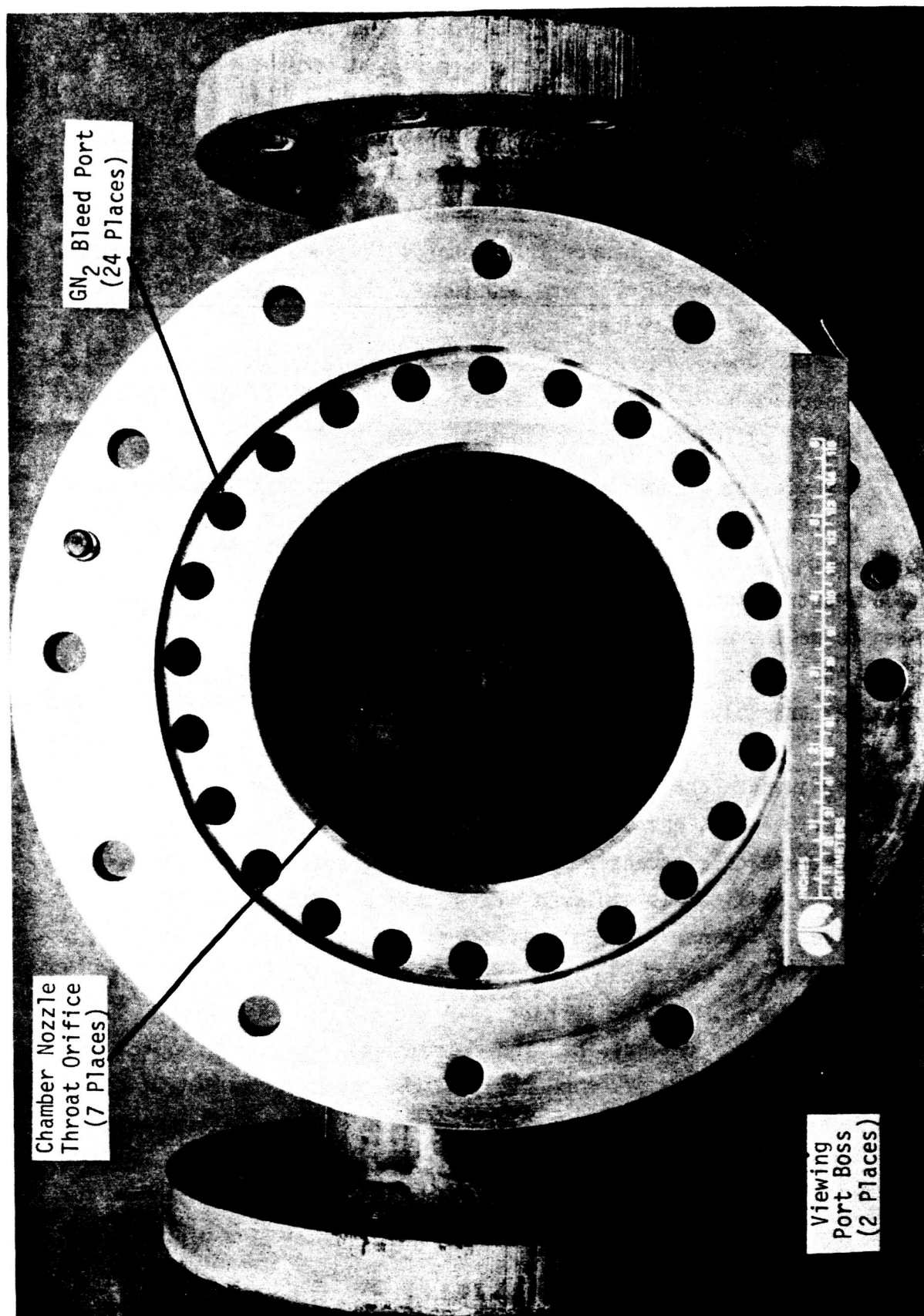
5AA34-10/29/74-S1B

Figure 4-5. High Contraction Ratio Tapered Chamber, View from Injector End Toward Nozzle

for obtaining the desired movies of the hot-firing experiments. The low contraction ratio cylindrical chamber was employed for the final 72 tests.

A photograph of the major combustor components for the low contraction ratio cylindrical chamber assembly is presented as Fig. 4-6 (Rocketdyne Engineering Drawing No. AP75-598). A schematic of the same assembly was presented as Fig.4-3. The chamber incorporates the same basic features as the high contraction ratio chamber (Section 4.2.1.1). However, there are several significant differences in design:

1. The chamber has a lower contraction ratio (~12 rather than ~77) and is cylindrical rather than tapered.

2. The viewing windows are mounted nearly flush to the chamber wall rather than being recessed ~10 cm (4-inch).

The lower contraction ratio and flush mounting of the viewing windows are believed to be the major reasons for reduced recirculation and thereby, increased ability to obtain better pictures of the impinging streams with this chamber assembly.

The inside diameter and length of the chamber were 8.99-cm (3.54-inch) and 30.5-cm (12-inch), respectively. The throat area (~5 cm^2) was the same as for the high contraction ratio chamber. However, a single centrally located orifice was employed rather than a distribution of several small orifices. Chamber material was 321 stainless steel.

As is evident upon inspection of Figs. 4-2 and 4-3, the portion of the injector assembly which extends into the chamber was machined to a smaller diameter (and tapered) in order to fit into the low contraction ratio chamber. In this configuration, all of the GN$_2$ bleed was injection in the annulus between the outside diameter of the portion of the injector which extends into the chamber and the chamber wall inside diameter. This area was sized to be the same as the GN$_2$ injection area of the high contraction ratio chamber assembly.

INJECTOR

VIEWING PORT
(TWO, 180° APART)

COMBUSTOR

WINDOW RETAINER FLANGES,
WINDOWS, AND SEALS
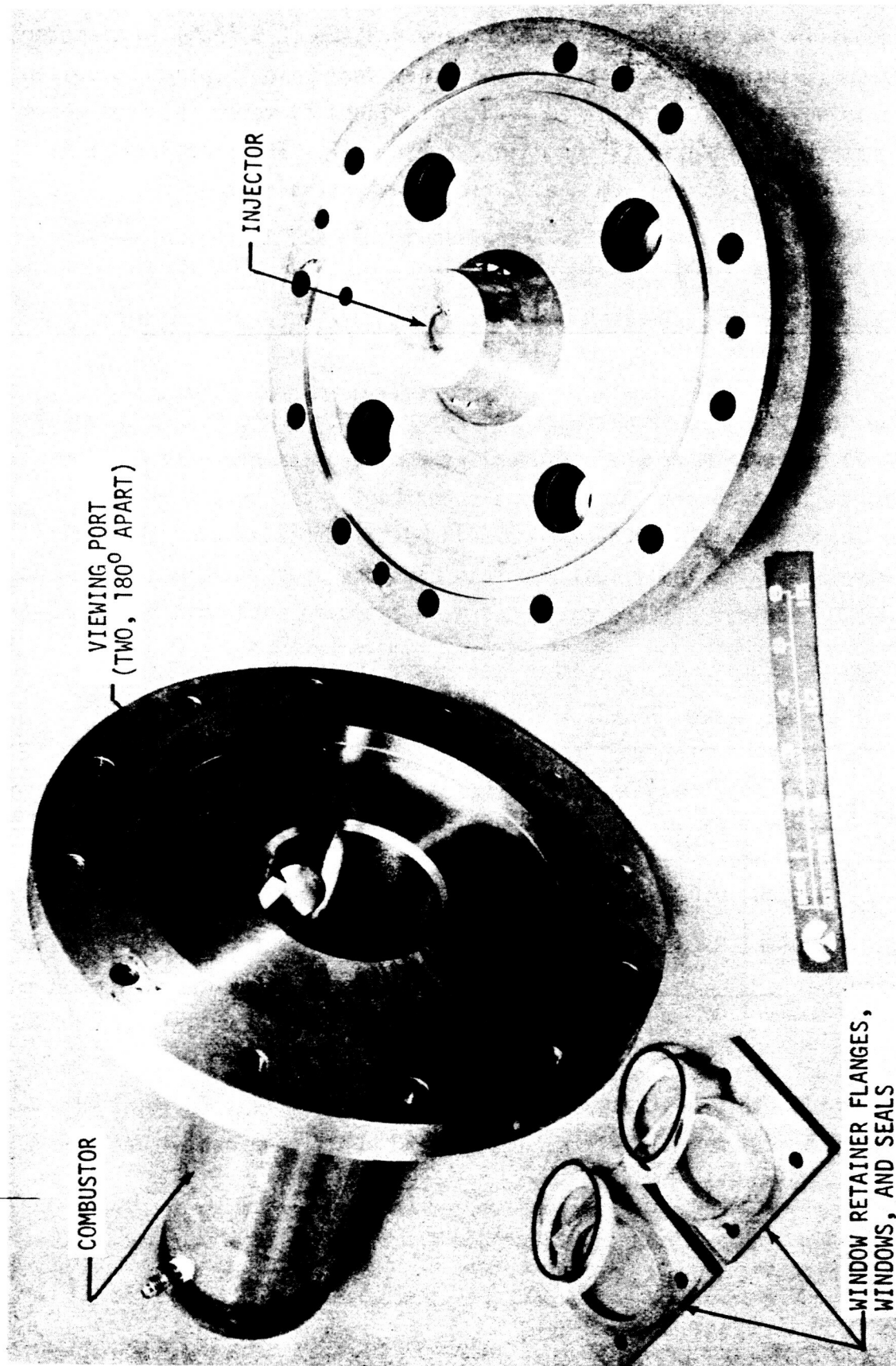
Figure 4-6. Photograph of Low Contraction Ratio Cylindrical Chamber Components

5DZ36-10/10/75-S1D

4-13

The windows in the cylindrical chamber were 6.35-cm (2.5-inch) in diameter by 1.27-cm (½-inch) thick quartz discs. They were held in place by bolted flanges in bosses which contained 5.08-cm (2-inch) diameter openings where the window cavity intersects the main chamber wall. The windows were located ~5-cm (2-inches) from the vertical combustion chamber centerline and provided a field of vision from the injector face ~3.8-cm (1½-inches) downstream of the element impingement points.

4.2.2 Injector

The injector, which is shown in Fig. 4-7 (front view) and 4-8 (back view) contains two separately-manifolded unlike-doublet elements, the impingement points of which are located on the horizontal centerline of the chamber approximately 0.9525-cm (0.375-inch) to either side of the vertical centerline. The individual doublets have the specifications presented in Table 4-2. Rounded orifice entrances were employed such that the doublet

TABLE 4-2. UNLIKE DOUBLET ELEMENT CONFIGURATIONS

Element Designation	Fuel Orifice Diameter		Oxidizer Orifice Diameter		Impingement Angle, Degrees	Orifice L/D	Impingement Distance L/D
	cm	Inch	cm	Inch			
UD-1	0.0508	0.020	0.061	0.024	60	12	~6
UD-2	0.0838	0.033	0.1016	0.040	60	12	~6

elements would exhibit stable coherent jet characteristics. The elements were fed by 0.475-cm (0.187-inch) downcomers. Only one doublet was connected during a given test.

4-14

Figure 4-7. Front Face of Injector
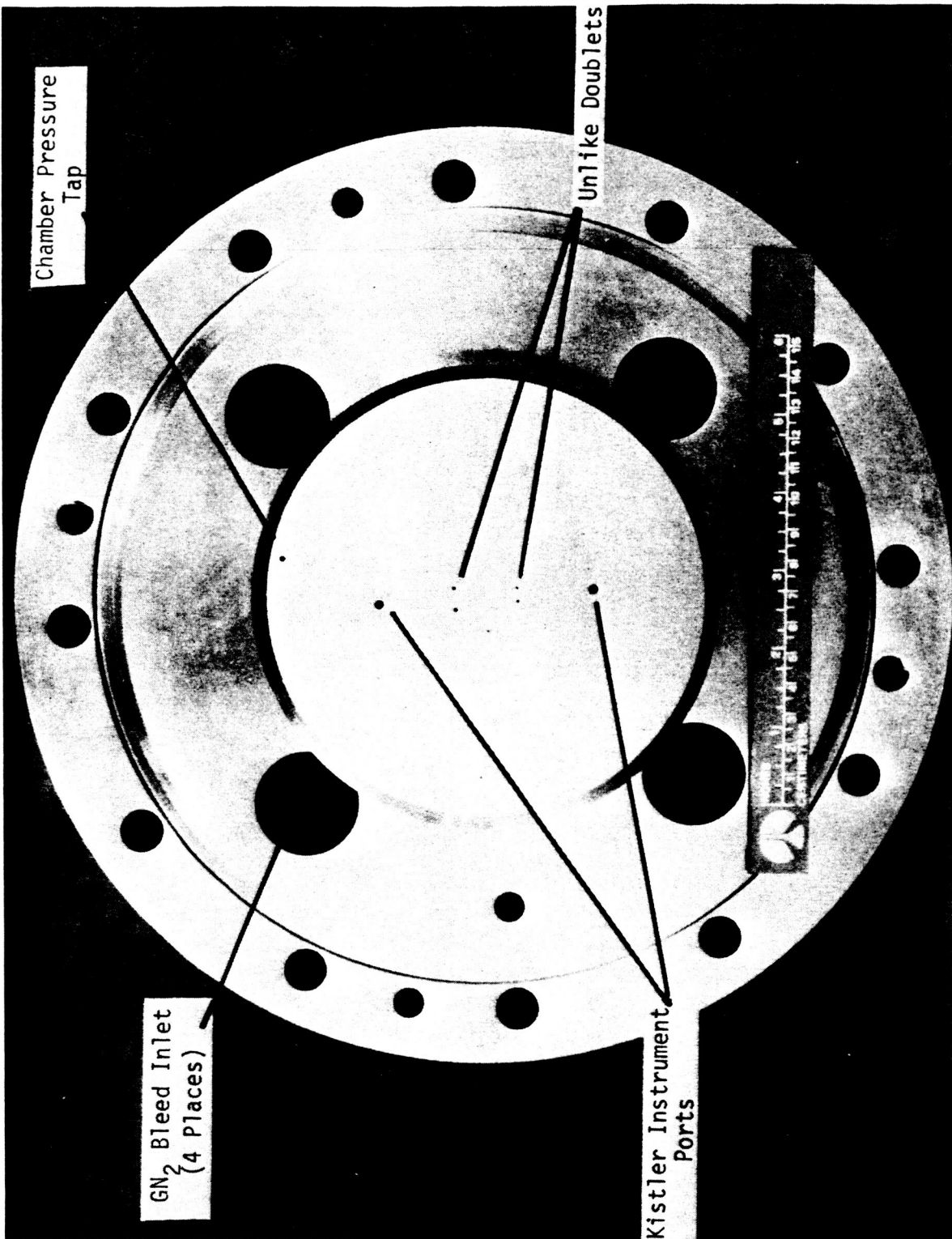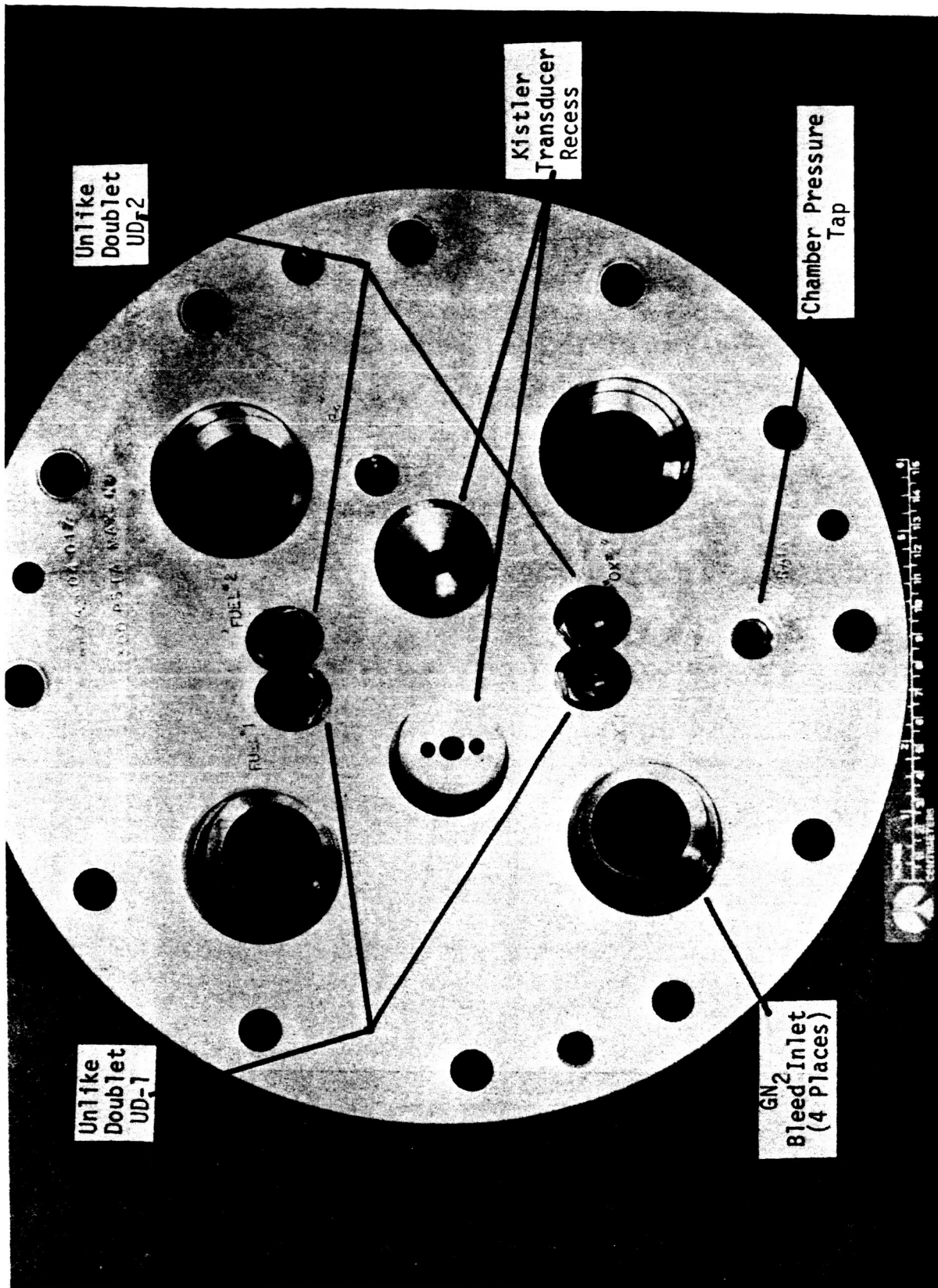
5AA34-10/29/74-S1A

Figure 4-8. Back Face of Injector

5AA34-10/29/74-S1C

Whereas previous investigations have usually studied doublets with equal fuel and oxidizer orifice diameters, the elements employed during this study were designed for optimum mixing at nominal engine mixture ratio. For an unlike-doublet element, the Rupe (Ref. 26) mixing criterion is

$$\frac{\rho_f \, d_f \, V_f^2}{\rho_{ox} \, d_{ox} \, V_{ox}^2} = 1.0 \tag{4-1}$$

which can alternately be expressed as

$$\left(\frac{1}{MR}\right)^2 \frac{\rho_{ox}}{\rho_f} \left(\frac{d_{ox}}{d_f}\right)^3 = 1.0 \tag{4-2}$$

Using Eq. (4-2) together with an average mixture ratio of 1.7 for N_2O_4/MMH and nominal propellant injection temperatures of 310 to 340°K (100 to 150°F) result in the orifice diameters shown in Table 4-2.

As is shown in Figs. 4-7 and 4-8, the injector is incorporated into a stainless steel end flange which also contains the GN_2 bleed manifold. Stainless steel was used not only for its compatibility with both the fuel and oxidizer but also because of its relatively low thermal conductivity compared to nickel or aluminum. The low thermal conductivity was necessary to prevent excessive heat loss from heated propellants to the injector body. Although all experiments were actually performed with the camera looking "edgewise" through the doublet spray fan, the symmetrical arrangement of the injector bolt circle would have permitted the elements to be rotated 90° relative to the viewing windows for alternate views of the unequal diameter doublet fans during hot-firing. Two locations were provided on the injector face for Kistler high-frequency crystal pressure transducers and an additional port was provided for chamber pressure measurement.

The injector is shown in Figs. 4-7 and 4-8 as it was used in the high contraction ratio chamber. The portion of the injector that extends into the chamber assembly was modified for use in the low contraction ratio chamber and the Kistler and chamber pressure ports were plugged for use in that chamber. Chamber pressure was measured on the fuel inlet port for the element not in use during tests conducted in the low contraction ratio chamber.

4.3 PHOTOGRAPHY

Motion pictures were taken of the doublet spray fan during each test using either a Millikan DBM 50AM camera at ~400 frames/sec or a Fastax at ~4000 frames/sec. In general, the lower frame speed was employed to reduce costs. Use of the lower speed film made it possible to conduct more tests in any given test slot. Fastax movies were taken in regions where cyclic "blowpart" was observed to better define the phenomenon. Eastman Kodak Ektachrome EF color film was employed for the first 158 tests and EFB color film was used for the remaining 113 experiements. The EF film is sensitive to daylight (sunlight) whereas EFB film is sensitive to a tungsten filament lamp. Backlight illumination was provided by a GE model BFJ 750 watt tungsten filament lamp and focused by a Fresnel lens at the photochamber window opposite the camera. A schematic of the photographic test setup is presented in Fig. 4-9. After experimentation during the early tests, most of the Millikan movies were made with an 18° shutter and an F stop setting of 11. Fastax movies were taken with a lens setting of F5.6. All photographs were taken with the camera looking "edgewise" through the doublet spray fan.

A photograph of the experiemental test apparatus on test stand Victor at PRA is presented as Fig. 4-10.
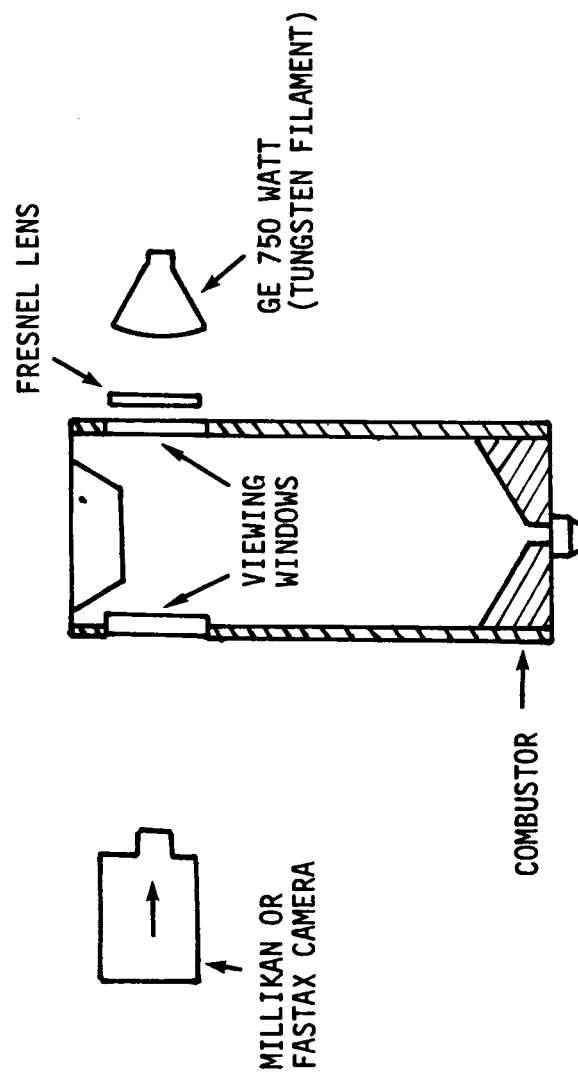
Figure 4-9. Schematic of Photographic Test Setup
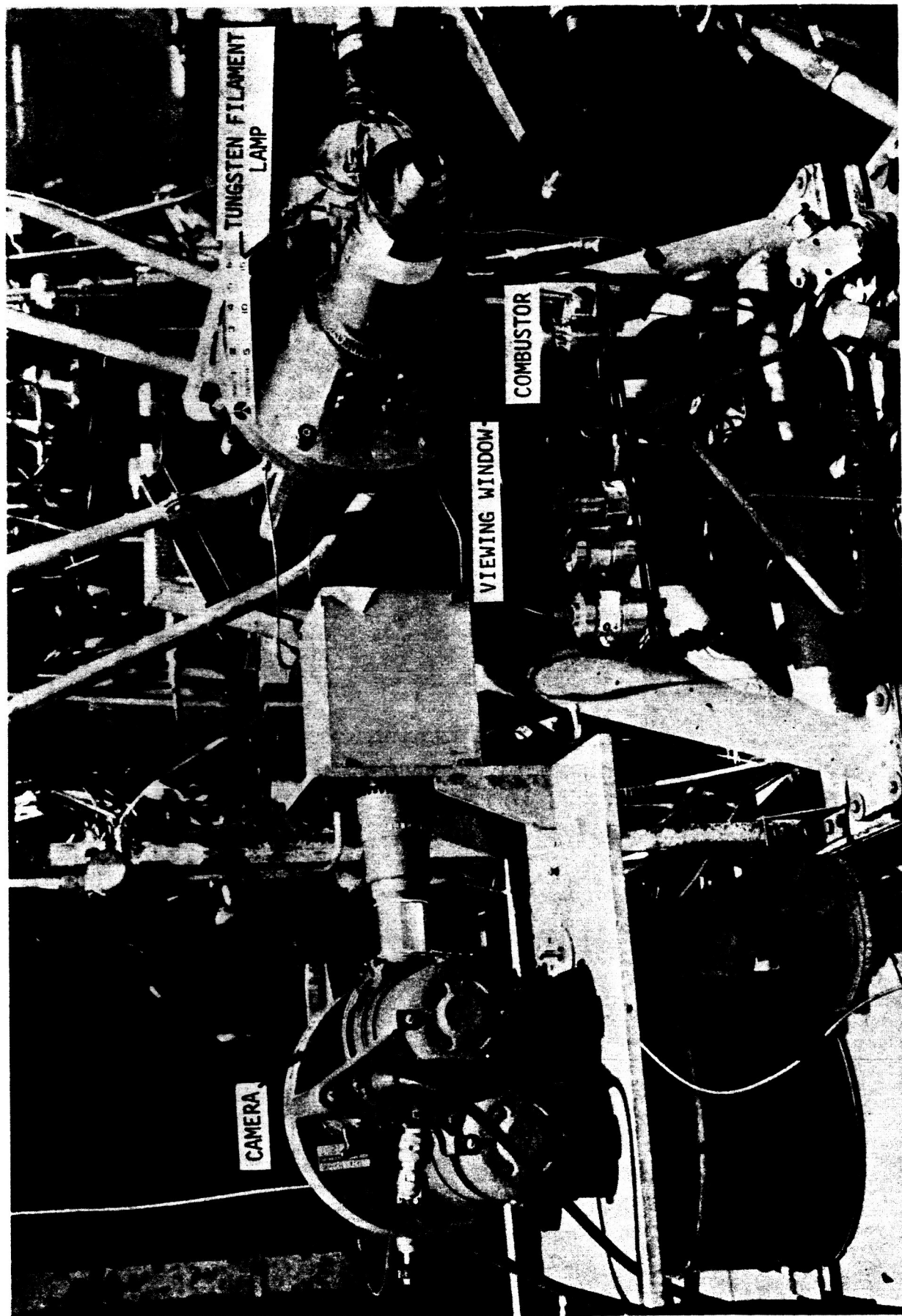
5ZA33-8/8/75-S1

Figure 4-10. Photograph of Experimental Test Apparatus

4-20

5.0 EXPERIMENTAL RESULTS

A total of 271 hot firing (N_2O_4/MMH) and 6 cold (water) flow experiments were conducted with unlike doublet elements UD-1 (d_f = 0.0508 cm; 0.020-inch) and UD-2 (d_f = 0.08382 cm; 0.033-inch). The test conditions/results of these tests are summarized in Tables 5-1 (hot-fire) and 5-2 (cold-flow). A brief discussion of these test results is presented in the following paragraphs. Detailed discussion and correlation of the results are presented in Section 6.0 (Discussion of Results).

5.1 HOT-FIRE EXPERIMENTS

Although a total of 271 hot-fire experiments were conducted, only 163 of these tests provided meaningful data in terms of reactive stream separation. Unsatisfactory films were obtained on a number of tests because recirculating N_2O_4 fumes and/or combustion gas products obscured the view of the spray fan. As was noted in Section 4.0, a modification of the chamber design was made to resolve this problem in the latter part of the program. The first 199 tests were conducted using the original high contraction ratio tapered chamber and the final 72 tests were conducted in a lower contraction ratio cylindrical chamber. The second (low contraction ratio) chamber design resolved the chamber gas recirculation problem.

The majority of the tests (202 of the 271) were conducted utilizing the UD-2 element. During these tests, chamber pressure was varied from an absolute pressure of 0.94 to ~15 atm (13.7 to 220 psia), fuel injection temperature from 283 to 400°K (50 to 260°F), oxidizer injection temperature from 283 to 322°K (50 to 120°F), and mixture ratio from ~1.2 to 2.5. Propellant injection velocities were varied from ~9 to 50 m/s (30 to 160 ft/sec). Tests conducted with the UD-1 element covered a smaller range of fuel injection velocity (~9 to 25 m/s; 30 to 80 ft/sec) and fuel injection temperature (283 to 350°K; 50 to 170°F).

Except for the variation in mixture ratio, the above variations in test parameters was planned. The mixture ratio was held as close to 1.7 (the

TABLE 5-1. SUMMARY OF DATA FOR N_2O_4/MMH REACTIVE STREAM SEPARATION EXPERIMENTS

Test No.	Element	Chamber Pressure $N/m^2 \times 10^{-6}$	Chamber Pressure psia	Mixture Ratio	Propellant Temperature Fuel °K	Fuel °F	Ox. °K	Ox. °F	Injection Velocity Fuel m/s	Fuel ft/sec	Ox. m/s	Ox. ft/sec	$\emptyset_{Mix}$	Film Quality (1)	Results (2)	Remarks
1-8	UD-1	-	-	-	-	-	-	-	-	-	-	-	-	-	-	Facility/system checkout tests
9		0.789	114	1.49	284	52	283	50	20.4	67	12.8	42	1.28	Sat.	M	-
10		0.865	125	1.53	284	52	282	49	19.8	65	12.8	42	1.22	Marg.	M	-
11		1.460	211	1.46	284	51	283	50	17.7	58	11.0	36	1.33	Unsat.	-	-
12		1.536	222	1.51	284	51	283	50	21.9	72	14.0	46	1.24	Unsat.	-	-
13		1.488	215	1.59	284	51	283	50	24.1	79	16.2	53	1.13	Unsat.	-	-
14		0.477	69	1.41	285	53	287	57	19.2	63	11.6	38	1.42	Unsat.	-	-
15		0.484	70	1.46	285	54	285	53	17.7	58	11.0	36	1.33	Unsat.	-	-
16		0.464	67	1.50	285	53	286	55	16.8	55	10.7	35	1.26	Unsat.	-	-
17		0.436	63	1.75	286	55	284	52	14.6	48	11.0	36	0.91	Sat.	M	-
18		0.429	62	1.94	286	56	283	50	13.4	44	10.7	35	0.78	Sat.	M	-
19		0.464	67	1.75	302	84	311	100	17.1	56	12.5	41	0.93	Sat.	M	Window cavity purging initiated.
20		0.477	69	1.79	302	84	318	114	17.7	58	12.8	42	0.92	Marg.	M	-
21		0.464	67	1.66	303	86	316	109	22.2	73	14.9	49	1.07	Marg.	M	-
22		0.789	114	1.68	304	88	302	84	16.4	54	11.3	37	1.03	Marg.	M	-
23		0.796	115	1.65	305	90	304	88	21.9	72	14.9	49	1.06	Marg.	M	-
24		1.149	166	1.50	304	88	313	104	15.2	50	11.6	38	1.06	Unsat.	-	-

(1) Index of film quality. In decreasing order of quality: Excellent, good, satisfactory, marginal, and unsatisfactory.
(2) Observed results: Mixed = M; Separated = S; Penetrated = P.

TABLE 5-1. (Continued)

Test No.	Element	Chamber Pressure $N/m^2 \times 10^{-6}$	Chamber Pressure psia	Mixture Ratio	Propellant Temperature Fuel °K	Fuel °F	Ox. °K	Ox. °F	Injection Velocity Fuel m/s	Fuel ft/sec	Ox. m/s	Ox. ft/sec	ρ_{Mix}	Film Quality (1)	Results (2)	Remarks
25	UD-1	1.481	214	1.57	306	92	312	103	14.0	46	11.3	37	0.96	Unsat.	-	-
26		2.000	289	1.78	309	97	315	107	14.3	47	11.0	36	0.88	Unsat.	-	-
27		0.768	111	2.01	315	107	324	124	16.8	55	14.6	48	0.69	Unsat.	-	-
28		0.754	109	1.82	320	117	322	120	17.4	57	13.7	45	0.84	Unsat.	-	-
29		0.782	113	1.46	-	-	305	90	14.0	46	7.9	26	1.44	Marg.	M	-
30		0.754	109	1.52	298	77	302	84	17.7	58	10.4	34	1.35	Marg.	M	-
31		0.823	119	1.69	316	109	300	81	20.1	66	13.1	43	1.10	Marg.	M	-
32		0.789	114	1.61	322	121	298	77	21.6	71	13.1	43	1.23	Marg.	M	-
33		1.183	171	1.72	308	95	297	76	13.7	45	9.1	30	1.05	Marg.	M	-
34		1.515	219	1.38	312	103	297	75	15.2	50	8.8	29	1.50	Unsat.	-	-
35		0.477	69	1.66	319	115	296	74	21.6	71	13.7	45	1.15	Marg.	M	-
36		0.775	112	1.66	318	113	296	74	17.1	56	10.7	35	1.17	Marg.	M	-
37		0.809	117	1.82	331	136	295	72	21.9	72	14.9	49	0.97	Marg.	M	-
38		1.121	162	1.84	326	128	296	73	15.2	50	10.7	35	0.92	Marg.	M	-
39		1.280	185	1.69	331	136	297	75	21.3	70	13.4	44	1.12	Marg.	M	-
40		1.515	219	1.54	330	134	295	72	15.8	52	10.0	33	1.23	Unsat.	-	-
41		1.771	256	1.85	336	145	296	73	19.5	64	14.6	48	0.86	Unsat.	-	-
42		2.014	291	1.60	334	142	296	73	16.8	55	11.0	36	1.15	Unsat.	-	-

(1) Index of film quality. In decreasing order of quality: Excellent, good, satisfactory, marginal, and unsatisfactory.
(2) Observed results: Mixed = M; Separated = S; Penetrated = P.

TABLE 5-1. (Continued)

Test No.	Element	Chamber Pressure $N/m^2 \times 10^{-6}$	Chamber Pressure psia	Mixture Ratio	Propellant Temperature Fuel °K	Fuel °F	Ox. °K	Ox. °F	Injection Velocity Fuel m/s	Fuel ft/sec	Ox. m/s	Ox. ft/sec	ρ_{Mix}	Film Quality (1)	Results (2)	Remarks
43	UD-2	0.477	69	1.86	318	114	305	89	14.3	47	11.0	36	0.84	Good	M	Erroneous fuel orifice ΔP calibration for tests 43-93.
44		0.477	69	1.79	318	114	305	89	15.2	50	11.3	37	0.92	Unsat.	-	-
45		0.491	71	1.51	320	117	305	90	17.7	58	10.7	35	1.32	Marg.	M	-
46		0.491	71	1.94	321	119	305	89	19.5	64	15.5	51	0.79	Sat.	M/S	-
47		0.844	122	1.96	316	110	303	86	13.7	45	11.0	36	0.77	Unsat.	-	-
48		0.844	122	1.53	320	116	302	84	17.1	56	10.4	34	1.30	Marg.	M/S	-
49		0.844	122	1.75	325	125	302	85	20.7	68	14.9	49	0.96	Sat.	S	-
50		0.844	122	1.71	327	129	302	85	21.6	71	14.6	48	1.05	Sat.	S	-
51		0.429	62	2.22	324	124	309	97	13.7	45	12.2	40	0.61	Good	M	-
52		0.782	113	2.08	315	107	310	98	13.7	45	11.6	38	0.68	Sat.	M	-
53		1.149	166	2.17	314	106	309	97	12.8	42	11.6	38	0.62	Unsat.	-	-
54		0.464	67	2.41	315	107	308	96	16.4	54	16.4	54	0.50	Marg.	M	-
55		0.789	114	2.29	322	121	311	101	17.4	57	15.8	52	0.58	Marg.	S	-
56		1.135	164	2.29	321	119	310	99	17.1	56	15.8	52	0.57	Marg.	M	-
57		1.467	212	2.25	317	112	310	98	12.8	42	11.9	39	0.58	Unsat.	-	-
58		1.502	217	2.20	320	116	309	97	17.1	56	15.2	50	0.61	Unsat.	-	-
59		0.443	64	2.09	328	131	311	100	13.7	45	11.0	36	0.72	Sat.	S	-

(1) Index of film quality. In decreasing order of quality: Excellent, good, satisfactory, marginal, and unsatisfactory.
(2) Observed results: Mixed = M; Separated = S; Penetrated = P.

TABLE 5-1. (Continued).

Test No.	Element	Chamber Pressure N/m² x10⁻⁶	Chamber Pressure psia	Mixture Ratio	Propellant Temperature Fuel °K	Fuel °F	Ox. °K	Ox. °F	Injection Velocity Fuel m/s	Fuel ft/sec	Ox. m/s	Ox. ft/sec	$\varnothing_{Mix}$	Film Quality (1)	Results (2)	Remarks
60	UD-2	0.782	113	2.37	337	147	310	98	18.3	60	11.0	36	0.55	Sat.	S	
61		1.481	214	2.26	331	137	310	98	28.0	92	25.9	85	0.58	Unsat.	-	
62		1.495	216	2.23	340	153	309	97	17.4	57	15.8	52	0.60	Unsat.	-	
63		0.443	64	2.22	346	164	310	99	19.2	63	16.2	53	0.65	Sat.	S	
64		0.789	114	2.36	340	153	310	99	13.4	44	11.9	39	0.58	Marg.	S	
65		0.789	114	2.51	346	164	312	103	12.2	40	12.2	40	0.48	Unsat.	-	
66		0.768	111	2.33	362	192	316	110	18.9	62	16.8	55	0.59	Marg.	S	
67	UD-1	0.429	62	1.64	308	95	312	103	16.8	55	11.6	38	1.05	Good	M	Window purging increased.
68		0.422	61	2.12	308	95	310	99	18.0	59	15.5	51	0.66	Sat.	M	
69		0.720	104	2.57	305	90	308	96	10.4	34	11.3	37	0.43	Sat.	M	
70		0.699	101	2.44	308	96	308	96	16.4	54	16.8	55	0.48	Good	M	
71		1.031	149	3.04	307	93	308	96	9.8	32	12.5	41	0.31	Unsat.	-	
72		1.066	154	2.63	309	97	306	91	14.0	46	15.5	51	0.41	Unsat.	-	
73		1.391	201	2.56	306	92	310	99	11.6	38	12.5	41	0.43	Unsat.	-	
74		0.408	59	2.23	304	87	309	97	12.8	42	13.7	45	0.50	Good	M	
75		0.733	106	2.22	306	92	306	92	12.2	40	11.9	39	0.55	Sat.	M	
76		0.720	104	2.44	309	97	304	88	15.8	52	15.2	50	0.51	Marg.	M	

(1) Index of film quality. In decreasing order of quality: Excellent, good, satisfactory, marginal, and unsatisfactory.
(2) Observed results: Mixed = M; Separated = S; Penetrated = P.

TABLE 5-1. (Continued)

Test No.	Element	Chamber Pressure		Mixture Ratio	Propellant Temperature				Injection Velocity				ϕ_{Mix}	Film Quality (1)	Results (2)	Remarks
		$N/m^2 \times 10^{-6}$	psia		Fuel		Ox.		Fuel		Ox.					
					°K	°F	°K	°F	m/s	ft/sec	m/s	ft/sec				
77	UD-1	1.066	154	2.51	308	96	304	88	12.2	40	12.8	42	0.45	Unsat.	-	-
78		1.412	204	2.30	310	98	304	87	15.8	52	15.2	50	0.54	Unsat.	-	-
79		1.398	202	2.56	315	107	304	87	14.3	47	15.2	50	0.44	Unsat.	-	-
80		1.813	262	2.36	316	110	302	85	11.3	37	11.3	37	0.51	Unsat.	-	-
81		1.813	262	2.43	318	113	303	86	15.5	51	15.8	52	0.48	Unsat.	-	-
82		0.429	62	2.27	311	101	307	93	13.1	43	11.3	37	0.61	Good	M	-
83		0.720	104	2.36	316	110	303	86	12.2	40	11.0	36	0.56	Sat.	M	-
84		1.066	154	2.42	324	123	304	88	11.6	38	11.0	36	0.52	Marg.	M	-
85		0.401	58	1.91	316	110	311	101	13.7	45	10.7	35	0.81	ExcInt	M	-
86		0.401	58	1.91	325	125	310	98	13.7	45	10.4	34	0.82	Good	M	-
87		0.401	58	1.93	331	137	309	97	13.7	45	10.4	34	0.83	Good	M	-
88		0.408	59	2.18	318	114	307	94	13.1	43	11.3	37	0.64	Good	M	-
89		0.443	64	2.27	328	132	307	94	12.5	41	11.0	36	0.60	Sat.	M	-
90		0.443	64	2.27	335	143	309	97	12.5	41	11.0	36	0.60	Sat.	M	-
91		0.408	59	2.15	331	137	307	94	18.3	60	15.2	50	0.67	Sat.	M	-
92		0.429	62	2.25	344	159	312	102	16.4	54	14.0	46	0.62	Sat.	M	-
93		0.429	62	2.22	351	172	312	103	16.4	54	14.0	46	0.63	Sat.	M	-
94-99	UD-2	-	-	-	-	-	-	-	-	-	-	-	-	-	-	Facility/system checkout tests.

(1) Index of film quality. In decreasing order of quality: Excellent, good, satisfactory, marginal, and unsatisfactory.
(2) Observed results: Mixed = M; Separated = S; Penetrated = P.

TABLE 5-1. (Continued)

Test No.	Element	Chamber Pressure		Mixture Ratio	Propellant Temperature				Injection Velocity				ø_Mix	Film Quality (1)	Results (2)	Remarks
					Fuel		Ox.		Fuel		Ox.					
		$N/m^2 \times 10^{-6}$	psia		°K	°F	°K	°F	m/s	ft/sec	m/s	ft/sec				
100	UD-2	0.173	25	1.61	299	78	296	73	18.0	59	12.2	40	1.12	Sat.	M	-
100A		0.214	31	1.84	298	78	296	74	17.7	58	13.4	44	0.86	Sat.	M	-
101		0.353	51	1.54	300	81	294	69	18.3	60	11.6	38	1.23	Marg.	M	-
101A		0.214	31	1.56	297	76	295	71	18.6	61	11.9	39	1.20	Marg.	M	-
102		0.512	74	1.73	300	81	296	74	16.8	55	11.9	39	0.98	Marg.	M	-
103		0.747	108	1.78	298	78	296	73	16.8	55	12.5	41	0.92	Good	M	-
104		0.782	113	1.76	299	79	296	74	23.2	76	17.1	56	0.94	Sat.	M	-
105		1.142	165	1.61	298	78	295	71	17.7	58	11.9	39	1.13	Sat.	M	-
106		0.235	34	1.76	305	90	296	73	16.2	53	11.6	38	0.95	Sat.	M	-
107		0.374	54	1.79	307	94	295	71	16.2	53	11.9	39	0.92	Sat.	M	-
108		0.512	74	1.64	313	104	295	71	17.7	58	11.9	39	1.10	Unsat.	-	Camera malfunction
109		0.768	111	1.78	312	102	294	69	15.8	52	11.6	38	0.94	Unsat.	-	
110		0.775	112	1.84	328	132	294	69	22.9	75	17.1	56	0.89	Unsat.	-	
111		1.114	161	1.81	320	117	293	68	16.4	54	12.2	40	0.91	Unsat.	-	
112		0.235	34	1.82	326	128	293	68	15.8	52	11.6	38	0.91	Unsat.	-	
113		0.360	52	1.82	332	138	292	67	16.2	53	11.6	38	0.92	Unsat.	-	
114		0.491	71	1.83	332	139	292	67	16.2	53	11.6	38	0.91	Unsat.	-	
115		0.761	110	1.70	339	151	292	66	16.8	55	11.3	37	1.06	Unsat.	-	

(1) Index of film quality. In decreasing order of quality: Excellent, good, satisfactory, marginal, and unsatisfactory.
(2) Observed results: Mixed = M; Separated = S; Penetrated = P.

TABLE 5-1. (Continued)

Test No.	Element	Chamber Pressure N/m²×10⁻⁶	Chamber Pressure psia	Mixture Ratio	Propellant Temperature Fuel °K	Fuel °F	Ox. °K	Ox. °F	Injection Velocity Fuel m/s	Fuel ft/sec	Ox. m/s	Ox. ft/sec	$\emptyset_{Mix}$	Film Quality (1)	Results (2)	Remarks
116	UD-2	0.768	111	1.78	345	161	291	65	23.5	77	16.4	54	0.97	Unsat.	-	Camera malfunction
117		1.121	162	1.84	341	155	291	64	15.8	52	11.6	38	0.91	Unsat.	-	
118		0.249	36	1.67	298	78	305	89	11.9	39	8.2	27	1.04	Sat.	M	—
119		0.353	51	1.78	300	81	304	88	10.7	35	7.9	26	0.92	Good	M	—
120		0.477	69	1.74	299	79	305	89	17.4	57	12.8	42	0.95	Good	M	—
121		0.754	109	1.73	299	78	308	96	16.4	54	11.9	39	0.96	Sat.	M	—
122		0.747	108	1.74	301	83	308	96	23.5	77	17.1	56	0.95	Sat.	M	—
123		1.107	160	1.75	301	82	308	96	16.4	54	12.2	40	0.94	Marg.	M	—
124		0.263	38	1.66	301	83	309	97	17.4	57	12.2	40	1.04	Sat.	M	—
125		0.311	45	1.64	302	84	310	99	23.8	78	16.4	54	1.07	Sat.	M	—
126		0.291	42	1.65	312	102	308	96	16.8	55	11.6	38	1.07	Sat.	M	—
127		0.353	51	1.66	320	116	309	97	17.4	57	11.9	39	1.06	Sat.	M	—
128		0.477	69	1.81	324	123	310	98	16.4	54	12.2	40	0.90	Sat.	S	—
129		0.747	108	1.68	327	130	310	98	16.8	55	11.6	38	1.05	Sat.	S	—
130		0.733	106	1.73	337	148	311	101	22.6	74	15.8	52	0.99	Sat.	S	—
131		1.107	160	1.81	333	140	311	100	15.5	51	11.6	38	0.90	Marg.	S	—
132		0.263	38	1.70	331	137	310	98	15.8	52	11.0	36	1.03	Sat.	S	—
133		0.311	45	1.70	335	143	311	101	22.6	74	15.5	51	1.03	Marg.	M	—

(1) Index of film quality. In decreasing order of quality: Excellent, good, satisfactory, marginal, and unsatisfactory.
(2) Observed results: Mixed = M; Separated = S; Penetrated = P.

TABLE 5-1. (Continued)

Test No.	Element	Chamber Pressure N/m²×10⁻⁶	Chamber Pressure psia	Mixture Ratio	Propellant Temperature Fuel °K	Fuel °F	Ox. °K	Ox. °F	Injection Velocity Fuel m/s	Fuel ft/sec	Ox. m/s	Ox. ft/sec	φ_Mix	Film Quality (1)	Results (2)	Remarks
134	UD-2	0.256	37	1.59	334	142	388	95	17.1	56	11.0	36	1.18	Sat	M	-
135		0.387	56	1.70	334	141	310	98	16.4	54	11.3	37	1.03	Sat.	S	-
136		0.477	69	1.73	340	152	312	103	16.8	55	11.6	38	1.00	Sat.	S	-
137		0.761	110	1.68	341	155	312	103	16.8	55	11.3	37	1.06	Marg.	S	-
138		0.733	106	1.71	348	168	315	107	23.2	76	15.8	52	1.03	Marg.	S	-
139		1.093	158	1.74	342	157	311	101	18.0	59	12.8	42	0.99	Marg.	S	-
140		0.277	40	1.65	341	155	292	66	16.8	55	11.0	36	1.13	Sat	S	-
141		0.270	39	1.66	349	169	291	75	16.4	54	10.7	35	1.12	Sat.	S	-
142		0.291	42	1.81	342	157	289	60	15.5	51	11.0	36	0.94	Sat.	S	-
143		0.360	52	1.84	351	172	285	54	15.2	50	11.0	36	0.92	Sat.	S	-
144		0.491	71	1.72	348	167	287	57	16.4	54	11.0	36	1.05	Sat.	S	-
145		0.498	72	1.73	352	175	285	53	16.2	53	10.7	35	1.05	Sat.	S	-
146-150		-	-	-	-	-	-	-	-	-	-	-	-	-	-	Facility/system checkout tests.
151		0.803	116	1.47	300	80	289	61	18.0	59	10.0	33	1.47	Sat.	M	-
152		0.782	113	1.68	292	67	287	57	46.6	153	29.6	97	1.14	Sat.	P	-
153		0.761	110	2.03	296	73	290	62	14.3	47	11.0	36	0.78	Unsat.	-	-
154		0.810	117	1.76	295	72	288	60	15.5	51	10.4	34	1.03	Sat.	M	-
155		0.816	118	1.60	295	72	288	59	23.2	76	14.0	46	1.25	Sat.	M	-

(1) Index of film quality. In decreasing order of quality: Excellent, good, satisfactory, marginal, and unsatisfactory.
(2) Observed results: Mixed = M; Separated = S; Penetrated = P.

TABLE 5-1. (Continued)

Test No.	Element	Chamber Pressure N/m²×10⁻⁶	Chamber Pressure psia	Mixture Ratio	Propellant Temperature Fuel °K	Fuel °F	Ox. °K	Ox. °F	Injection Velocity Fuel m/s	Fuel ft/sec	Ox. m/s	Ox. ft/sec	ϕ_{Mix}	Film Quality (1)	Results (2)	Remarks
156	UD-2	0.816	118	1.72	295	71	287	58	28.0	92	17.7	58	1.12	Sat.	M/P	-
157		1.495	216	1.69	295	71	286	56	12.8	42	7.9	26	1.16	Unsat.	-	-
158		1.495	216	1.85	292	67	284	51	17.4	57	12.2	40	0.93	Unsat.	-	-
159		0.560	81	1.79	293	68	286	55	25.6	84	17.4	57	1.00	Sat.	M	-
160		0.823	119	1.64	290	62	284	51	33.8	111	21.0	69	1.19	Sat.	P	-
161		0.823	119	1.66	289	61	281	47	38.4	126	24.1	79	1.16	Sat.	P	-
162		0.754	109	1.62	294	69	281	46	48.2	158	29.3	96	1.23	Sat.	P	-
163		0.567	82	1.65	290	63	281	47	38.4	126	24.1	79	1.17	Sat.	M/P	-
164		1.529	221	1.72	292	67	284	52	21.9	72	14.3	47	1.08	Unsat.	-	-
165		1.529	221	1.65	290	63	283	50	29.9	98	18.6	61	1.18	Unsat.	-	-
166		0.775	112	1.79	342	156	288	59	15.2	50	10.7	35	0.96	Unsat.	-	-
167		0.796	115	1.98	348	167	286	56	12.2	40	9.4	31	0.79	Unsat.	-	-
168		0.789	114	1.66	354	177	286	56	14.6	48	9.4	31	1.13	Unsat.	-	-
169		-	-	-	-	-	-	-	-	-	-	-	-	-	-	Fuel main valve did not open
170		0.775	112	1.29	350	171	292	67	18.3	60	9.1	30	1.87	Unsat.	-	-
171		0.789	114	1.32	354	177	291	64	17.1	56	8.8	29	1.79	Unsat.	-	-
172	↓	0.823	119	1.49	359	187	292	66	14.3	47	8.2	27	1.40	Unsat.	-	-
173		0.823	119	1.52	365	197	291	65	13.4	44	7.9	26	1.36	Unsat.	-	-

(1) Index of film quality. In decreasing order of quality: Excellent, good, satisfactory, marginal, and unsatisfactory.
(2) Observed results: Mixed = M; Separated = S; Penetrated = P.

5-10

TABLE 5-1. (Continued)

Test No.	Element	Chamber Pressure N/m²×10⁻⁶	Chamber Pressure psia	Mixture Ratio	Propellant Temperature Fuel °K	Fuel °F	Ox. °K	Ox. °F	Injection Velocity Fuel m/s	Fuel ft/sec	Ox. m/s	Ox. ft/sec	∅Mix	Film Quality (1)	Results (2)	Remarks
174	UD-2	0.789	114	1.39	382	228	291	65	29.0	95	15.2	50	1.65	Unsat.	-	-
175		0.796	115	1.60	385	234	291	65	28.3	93	17.1	56	1.25	Unsat.	-	-
176		0.768	111	1.60	389	240	292	66	34.4	113	20.7	68	1.25	Unsat.	-	-
177		0.823	119	1.67	388	239	291	65	32.3	106	20.1	66	1.16	Unsat.	-	-
178		0.775	112	1.68	395	252	293	68	46.6	153	29.3	96	1.16	Unsat.	-	-
179		0.823	119	1.65	399	258	292	66	46.6	153	28.6	94	1.19	Unsat.	-	-
180		0.782	113	1.33	357	183	315	107	15.8	52	8.5	28	1.71	Unsat.	-	-
181		0.775	112	2.65	367	201	315	107	17.1	56	18.0	59	0.44	Unsat.	-	-
182		0.775	112	3.33	363	194	313	104	14.3	47	18.9	62	0.28	Unsat.	-	-
183		0.823	119	0.98	381	226	321	118	26.8	88	10.4	34	3.21	Unsat.	-	-
184		0.754	109	1.27	306	92	297	75	14.9	49	7.9	26	1.82	Unsat.	-	-
185		0.796	115	1.47	341	155	295	72	12.5	41	7.3	24	1.41	Unsat.	-	-
186		0.740	107	2.38	311	101	296	73	8.8	29	8.8	29	0.52	Unsat.	-	-
187		0.747	108	1.66	342	157	295	71	12.8	42	8.2	27	1.11	Unsat.	-	-
188		0.754	109	1.61	326	128	295	72	14.0	46	9.1	30	1.16	Unsat.	-	-
189		0.761	110	1.57	357	183	295	71	14.3	47	8.8	29	1.26	Unsat.	-	-
190		0.747	108	1.27	300	80	298	77	14.0	46	7.3	24	1.80	Unsat.	-	-
191		0.747	108	1.23	298	77	296	74	14.0	46	7.0	23	1.94	Unsat.	-	-

(1) Index of film quality. In decreasing order of quality: Excellent, good, satisfactory, marginal, and unsatisfactory.
(2) Observed results: Mixed = M; Separated = S; Penetrated = P.

TABLE 5-1. (Continued)

Test No.	Ele-ment	Chamber Pressure N/m²×10⁻⁶	Chamber Pressure psia	Mixture Ratio	Propellant Temperature Fuel °K	Fuel °F	Ox. °K	Ox. °F	Injection Velocity Fuel m/s	Fuel ft/sec	Ox. m/s	Ox. ft/sec	$\emptyset_{Mix}$	Film Quality (1)	Results (2)	Remarks
192	UD-2	0.761	110	1.46	294	70	292	66	14.0	46	8.5	28	1.36	Unsat.	-	-
193		0.789	114	1.47	294	70	292	66	13.4	44	7.9	26	1.36	Unsat.	-	-
194		0.740	107	1.75	294	69	294	69	11.6	38	8.5	28	0.94	Unsat.	-	-
195		0.740	107	1.66	294	69	294	69	11.6	38	7.9	26	1.05	Unsat.	-	-
196		0.754	109	1.76	294	69	294	69	11.6	38	8.5	28	0.94	Unsat.	-	-
197		0.754	109	1.67	294	69	294	69	11.6	38	7.9	26	1.05	Unsat.	-	-
198		0.754	109	1.70	292	66	292	66	12.2	40	8.5	28	1.01	Unsat.	-	-
199		0.754	109	1.52	292	66	292	66	12.5	41	7.9	26	1.26	Unsat.	-	-
200		~1.04	~150	2.35	296	73	300	80	17.1	56	16.8	55	0.52	-	-	Observed test on TV monitor. First test conducted with low contraction chamber.
201		0.823	119	1.40	295	72	301	82	27.7	91	16.4	54	1.48	ExcInt	P	Tests 200-271 conducted with low contraction ratio chamber
202		0.789	114	1.51	294	69	301	83	29.0	95	18.3	60	1.26	Good	M/P	
203		0.782	113	1.45	293	68	301	83	30.2	99	18.3	60	1.37	ExcInt	P	
204		0.789	114	1.22	291	65	303	86	27.7	91	14.3	47	1.91	Good	M	
205		1.522	220	1.15	295	72	303	86	28.6	94	14.0	46	2.17	Good	P	
206		1.481	214	1.40	296	73	303	86	20.7	68	12.2	40	1.47	Good	M/P	
207		1.508	218	1.73	296	73	303	86	20.1	66	14.6	48	0.96	-	-	Observed test on TV monitor.System checkout
208		0.775	112	1.28	300	80	297	76	30.2	99	16.2	53	1.79	Good	P	-
209		0.789	114	1.65	299	78	295	72	27.1	89	18.6	61	1.08	Good	P	-

(1) Index of film quality. In decreasing order of quality: Excellent, good, satisfactory, marginal, and unsatisfactory.
(2) Observed results: Mixed = M; Separated = S; Penetrated = P.

TABLE 5-1. (Continued)

Test No.	Element	Chamber Pressure N/m²×10⁻⁶	psia	Mixture Ratio	Propellant Temperature Fuel °K	°F	Ox. °K	°F	Injection Velocity Fuel m/s	ft/sec	Ox. m/s	ft/sec	Ø Mix	Film Quality (1)	Results (2)	Remarks
210	UD-2	0.789	114	1.80	299	78	295	72	27.1	89	20.1	66	0.90	Good	P	
211		0.741	107	1.80	298	77	297	75	47.8	157	36.0	118	0.89	Marg.	P	
212		0.789	114	1.87	295	72	294	69	46.3	152	36.3	119	0.83	Marg.	P	
213		0.803	116	1.73	295	72	294	70	34.7	114	25.0	82	0.98	Marg.	P	
214		0.789	114	1.72	297	75	295	72	23.2	76	16.5	54	0.98	Sat.	M	
215		0.789	114	1.63	296	73	295	71	18.6	61	12.8	42	1.09	Good	M	
216		0.796	115	1.27	294	70	292	67	20.1	66	10.7	35	1.82	ExcInt	M	
217		0.796	115	1.25	295	72	294	69	19.5	64	10.1	33	1.86	Sat.	M	
218		0.789	114	1.25	297	75	296	73	19.2	63	10.1	33	1.86	Sat.	M	
219		0.789	114	1.37	298	77	297	76	17.4	57	10.1	33	1.56	Marg.	M	
220		1.495	216	1.52	300	80	297	75	17.1	56	10.7	35	1.26	Marg.	M	
221		1.515	219	1.69	299	79	297	76	21.6	71	15.2	50	1.02	Marg.	M	
222		1.529	221	1.82	300	81	298	77	28.6	94	21.6	71	0.88	Sat.	P	
223		1.508	218	1.82	301	82	299	78	27.1	89	20.7	68	0.88	Sat.	P	
224		1.495	216	1.60	300	81	299	78	34.7	114	23.2	76	1.14	Sat.	P	
225		1.467	212	1.72	300	81	298	77	44.2	145	31.7	104	0.99	Sat.	P	
226		0.519	75	1.70	299	78	296	74	17.1	56	12.2	40	1.01	Sat.	M	
227		0.505	73	1.57	299	78	297	75	24.1	79	15.8	52	1.18	Unsat.	-	

(1) Index of film quality. In decreasing order of quality: Excellent, good, satisfactory, marginal, and unsatisfactory.
(2) Observed results: Mixed = M; Separated = S; Penetrated = P.

TABLE 5-1.   (Continued)

Test No.	Element	Chamber Pressure $N/m^2 \times 10^{-6}$	psia	Mixture Ratio	Propellant Temperature Fuel °K	°F	Ox. °K	°F	Injection Velocity Fuel m/s	ft/sec	Ox. m/s	ft/sec	ϕ_{Mix}	Film Quality (1)	Results (2)	Remarks
228	UD-2	0.484	70	1.58	300	81	299	78	30.2	99	19.8	65	1.17	Marg.	M	
229		0.484	70	1.71	299	79	297	76	27.7	91	19.8	65	1.00	Marg.	M	
230		0.512	74	1.76	299	78	296	74	32.6	107	23.8	78	0.94	Marg.	M	
231		0.484	70	1.71	299	78	297	75	44.2	145	31.4	103	1.00	Unsat.	-	
232		0.775	112	1.70	296	73	295	72	17.1	56	12.2	40	1.01	Good	M	
233		0.754	109	1.37	295	72	294	70	11.6	38	6.7	22	1.56	Good	M	
234		0.747	108	1.65	295	72	294	69	12.5	41	8.5	28	1.07	Good	M	
235		1.453	210	1.67	295	71	294	69	11.6	38	7.9	26	1.04	Sat.	M	
236		1.502	217	1.93	294	69	293	68	11.0	36	8.8	29	0.78	Unsat.	-	
237		0.498	72	1.98	294	69	292	66	11.0	36	8.8	29	0.74	Unsat.	-	
238		0.484	70	1.89	293	68	291	65	10.7	35	8.5	28	0.82	Good	M	
239		0.768	111	1.76	294	70	292	67	11.6	38	8.5	28	0.94	Marg.	M	
240		0.858	124	1.66	290	63	292	66	27.1	89	18.9	62	1.06	ExcInt	M/P	
241		0.796	115	1.78	289	61	290	63	44.8	147	33.2	109	0.92	ExcInt	P	
242		0.525	76	1.61	291	64	290	62	48.2	158	32.3	106	1.13	Good	P	
243		0.526	76	1.56	292	66	292	67	28.6	94	18.9	62	1.19	Good	M/P	
244		0.512	74	1.59	292	67	291	64	13.1	43	8.8	29	1.15	Good	M	
245		0.512	74	1.69	292	66	291	65	12.5	41	8.8	29	1.02	-	-	Observed test on TV monitor. System checkout.

(1) Index of film quality. In decreasing order of quality: Excellent, good, satisfactory, marginal, and unsatisfactory.
(2) Observed results: Mixed = M; Separated = S; Penetrated = P.

TABLE 5-1. (Continued)

Test No.	Element	Chamber Pressure N/m²×10⁻⁶	Chamber Pressure psia	Mixture Ratio	Propellant Temperature Fuel °K	Fuel °F	Ox. °K	Ox. °F	Injection Velocity Fuel m/s	Fuel ft/sec	Ox. m/s	Ox. ft/sec	$\emptyset_{Mix}$	Film Quality (1)	Results (2)	Remarks
246	UD-2	0.519	75	1.80	295	72	294	70	11.6	38	8.8	29	0.89	Good	M	-
247		0.789	114	1.69	295	71	293	68	12.5	41	8.8	29	1.02	Good	M	-
248		1.418	205	1.81	295	71	293	68	12.5	41	9.4	31	0.89	Sat.	M	-
249		0.526	76	1.59	294	69	296	73	47.8	157	32.0	105	1.14	Good	P	-
250		0.796	115	1.59	294	70	296	73	47.8	157	32.0	105	1.14	Good	P	-
251		1.481	214	1.63	295	71	295	72	47.8	157	32.6	106	1.10	Good	P	-
252		0.505	73	1.67	295	72	295	71	28.0	92	19.5	64	1.04	Good	M	-
253		1.474	213	1.66	295	71	294	70	28.0	92	19.2	63	1.06	Good	P	-
254		0.810	117	1.35	296	73	299	78	44.8	147	25.3	83	1.59	Good	S	-
255		0.789	114	1.77	372	211	297	76	45.1	148	30.8	101	1.00	Good	S	-
256		0.823	119	1.60	370	207	297	75	36.6	120	22.6	74	1.22	Good	P	-
257		0.775	112	1.43	314	105	296	74	45.1	148	26.2	86	1.45	Good	P	-
258		0.823	119	1.37	301	83	321	118	44.8	147	26.2	86	1.52	Good	P	-
259		0.789	114	1.45	309	96	309	96	29.3	96	18.0	59	1.37	ExcInt	M/P	-
260		0.726	105	1.60	306	92	309	96	47.8	157	32.0	105	1.14	ExcInt	P	-
261		1.481	214	1.65	302	85	309	96	46.0	151	32.0	105	1.06	Good	P	-
262		0.761	110	1.26	306	92	309	96	16.5	54	8.5	28	1.82	Good	-	Camera on too soon.
263		0.761	110	1.57	307	93	309	96	15.5	51	10.1	33	1.18	Good	-	Steady fuel flow not established.

(1) Index of film quality. In decreasing order of quality: Excellent, good, satisfactory, marginal, and unsatisfactory.
(2) Observed results: Mixed = M; Separated = S; Penetrated = P.

TABLE 5-1. (Concluded)

Test No.	Element	Chamber Pressure N/m²×10⁻⁶	Chamber Pressure psia	Mixture Ratio	Propellant Temperature Fuel °K	Fuel °F	Ox. °K	Ox. °F	Injection Velocity Fuel m/s	Fuel ft/sec	Ox. m/s	Ox. ft/sec	ϕ_{Mix}	Film Quality (1)	Results (2)	Remarks
264	UD-2	1.481	214	1.77	302	84	310	98	15.5	51	11.6	38	0.91	Good	-	Camera on too soon. Steady fuel flow not established.
265		0.768	111	1.70	371	209	309	97	15.2	50	10.1	33	1.07	Good	S	
266		1.481	214	1.84	398	257	309	97	15.8	52	11.0	36	0.94	Good	S	
267		0.872	126	1.80	327	130	308	95	46.0	151	33.8	111	0.92	Sat.	S/P	
268		0.095	*13.8	1.76	312	102	306	92	45.1	148	32.9	108	0.94	Exclnt	M	
269		0.095	*13.8	1.63	311	101	306	91	29.6	97	20.1	66	1.09	Exclnt	M	
270		0.095	*13.8	1.39	306	92	302	85	15.5	51	8.8	29	1.51	Exclnt	-	Camera on too soon. Steady fuel flow not established.
271		0.095	*13.8	1.54	305	90	304	87	16.4	54	10.4	34	1.22	Exclnt	M	

*Open air tests.
(1) Index of film quality. In decreasing order of quality: Excellent, good, satisfactory, marginal and unsatisfactory.
(2) Observed results: Mixed = M; Separated = S; Penetrated = P.

TABLE 5-2. SUMMARY OF TEST CONDITIONS FOR COLD-FLOW (H_2O) TESTS*

Test No.	Injector	ϕ	Momentum Ratio, Fuel to Oxidizer	Injector ΔP Oxidizer $N/m^2 \times 10^{-6}$	psi	Fuel $N/m^2 \times 10^{-6}$	psi	Mixture Ratio H.F.	C.F.	Injection Velocity Oxidizer H.F. m/sec	ft/sec	C.F. m/sec	ft/sec	Fuel H.F. m/sec	ft/sec	C.F. m/sec	ft/sec
1	UC-2	0.96	0.79	0.166	24	0.187	27	1.75	1.36	9.8	32	11.6	38	13.4	44	12.5	51
2		0.95	0.78	0.726	105	0.844	122	1.76	1.36	20.7	68	24.9	81	28.3	93	26.5	87
3		0.97	0.80	1.937	280	2.277	329	1.75	1.36	33.5	110	40.5	133	46.6	153	43.3	142
4		0.94	0.78	0.208	30	0.235	34	1.75	1.38	11.0	36	13.1	43	14.9	49	14.5	48
5	UC-1	0.85	0.71	0.865	125	0.872	126	1.82	1.43	22.6	74	26.8	88	30.0	98	27.1	89
6		0.80	0.67	0.270	39	0.270	39	1.87	1.45	12.5	41	15.2	50	15.8	52	14.9	49

*Open air tests. Where only one column appears below a parameter, cold-flow and
simulated hot-fire conditions are similar. H.F. = Hot fire value simulated.
C.F. = Actual cold-flow value.

equal volume value for the N_2O_4/MMH propellant combination) as possible; however, because of limitations on the accuracy of the pressure regulators on the tanks, mixture ratio varied between ~1.5 and 1.9 for most of the tests. Unfortunately, during Tests 43-93 an erroneous calibration of the fuel orifice ΔP transducer resulted in operation at fuel flowrates lower than desired (i.e., high mixture ratio). The mixture ratios shown in Table 5-1 for these tests are the correct values.

As was noted in Section 4.0, the unlike-doublet elements were designed for optimum mixing at a mixture ratio of 1.7 based on the Rupe mixing criteria (Ref. 26) defined as

$$\phi = \frac{\rho_f \, V_f^2 \, d_f}{\rho_{ox} \, V_{ox}^2 \, d_{ox}} = \left(\frac{1}{MR}\right)^2 \left(\frac{d_{ox}}{d_f}\right)^3 \left(\frac{\rho_{ox}}{\rho_f}\right) = 1.0 \tag{5-1}$$

A value of $\phi = 1.0$ will give optimum mixing for an unlike-doublet element. To achieve the objectives of this program it was considered satisfactory to control ϕ between ~0.8 and 1.25, as was accomplished for the majority of the tests. Values of ϕ for each test are presented in Table 5-1.

5.1.1 Film Quality

Analysis of the color motion pictures provided the means of determining the occurrence of reactive stream separation. The readability of the films were divided into five categories: excellent, good, satisfactory, marginal and unsatisfactory. The results of this classification are shown in Table 5-1 for each test. As was noted previously, many unsatisfactory or marginal films were obtained in the initial (high contraction ratio) chamber due to combustor gas recirculation. In general, film quality decreased with increasing chamber pressure.

5.1.2 Occurrence of Separation

The tests in which marginal or better films were obtained were divided into several categories: mixed, separated, penetrated, or a combination of the above. Mixed tests were those in which no reactive stream separation was apparent. Two different types of reactive stream separation phenomenon were observed. One of these, termed penetration, was observed at high injection velocities with ambient temperature propellants. In this case, a portion of the fuel stream appeared to penetrate through or go around the oxidizer stream. The other phenomena, termed separation, was observed with heated propellants. The fuel and oxidizer streams appeared to blowapart and/or separate starting at some point downstream of the impingement point and progress backward to the impingement point when this phenomena was observed. In both cases, the observed reactive stream separation phenomena consisted of repeated pulses (i.e., it was cyclic). However, the pulsing did not exhibit the strength necessary to either disrupt the doublet jets upstream of the impingement point or to completely destroy the spray fan downstream of the impingement point; i.e., there were no instances of energetic stream blowapart or "popping" observable in the film data. Similarly, there were no occurrences of any pressure spiking on the oscillograph records of the Kistler crystal transducers located in the chamber or in the propellant manifolds. Use of these transducers was discontinued after approximately 100 tests.

It should be noted that in many of the tests where reactive stream separation was observed a clear distinction could not be made as to whether the phenomena was "separation" or "penetration". Since the two phenomenon appear to be driven by different mechanisms, as will be noted in Section 6.0 (Discussion of Results), the basis of selection for terminology was based on whether the tests were conducted at high injection velocity (termed penetration) or with heated fuel (termed separation). The method of selection of the category (mixed, separated, or penetrated) is qualitative and subjective. Consequently, in some cases a combined result such as mixed/separated or separated/penetrated is reported. The category for each test is presented in the next to last column of Table 5-1.

Photographs of two tests, one mixed and one penetrated, are presented
in Fig. 5-1 to illustrate the phenomenon observed. The test number and
test conditions are noted on the figure.

5.1.3 Correlation of Separation/Penetration
to Operating Variables

The hot-fire data were plotted as functions of the primary operating
variables (chamber pressure, fuel injection velocity, and fuel injec-
tion temperature) to gain insight into possible mechanisms for the
separation/penetration phenomenon. Plots of chamber pressure versus
fuel injection velocity and fuel injection temperature were made for
both injector elements.

No separation or penetration was observed on any of the tests conducted
with the UD-1 element. Data plots for this element are still presented
however to clearly illustrate the range over which the test parameters
were varied with this element. Aerojet (Ref. 27) observed separation
and/or penetration with an element similar to the UD-1 element (Contract
NAS9-14186) when they conducted tests at higher chamber pressure, propel-
lant injection velocities, and fuel temperatures then were investigated
in this study. Aerojet's data will be correlated with this data in the
following section of this report (Section 6.0).

Figures 5-2 and 5-3 present plots of chamber pressure versus fuel injection
velocity for the UD-1 and UD-2 elements, respectively. Data are presented
only for the tests conducted with ambient temperature fuel ($T_f < \sim 316^{\circ}K$;
$110^{\circ}F$) for the UD-2 element so that the velocity and temperature effects
may be separated. Over the range of test parameters studied, no reactive
stream separation was observed with the UD-1 element. Penetration was ob-
served with the UD-2 element at the higher injection velocities and higher
chamber pressures. It appears that both chamber pressure and injection
velocity have a significant effect on reactive stream separation for the
UD-2 element. Since most of the tests were conducted at nearly the same
mixture ratio (~ 1.7), the data could have been plotted versus oxidizer in-
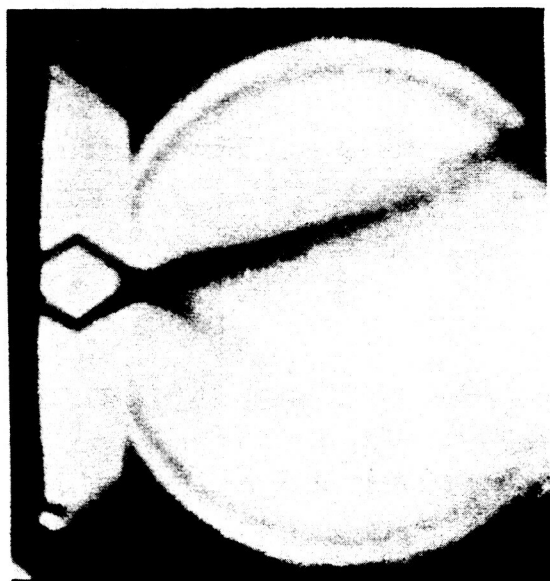jection velocity with similar results.
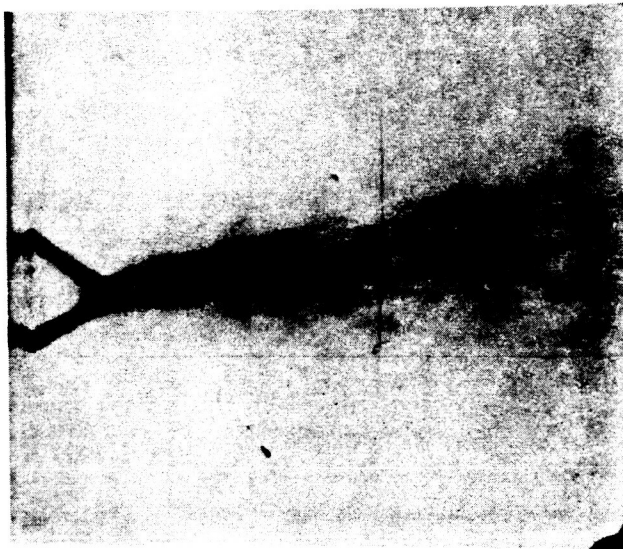
Test No. - 51

  Element - UD-2

   P_c - 0.429 x 10^6 N/M^2
        (62 psia)

   V_f - 13.7 m/s
        (45 ft/sec)

   T_f - 324°K
        (124°F)

A.   Mixed Test Condition

Test No. - 203

  Element - UD-2

   P_c - 0.782 x 10^6 N/M^2
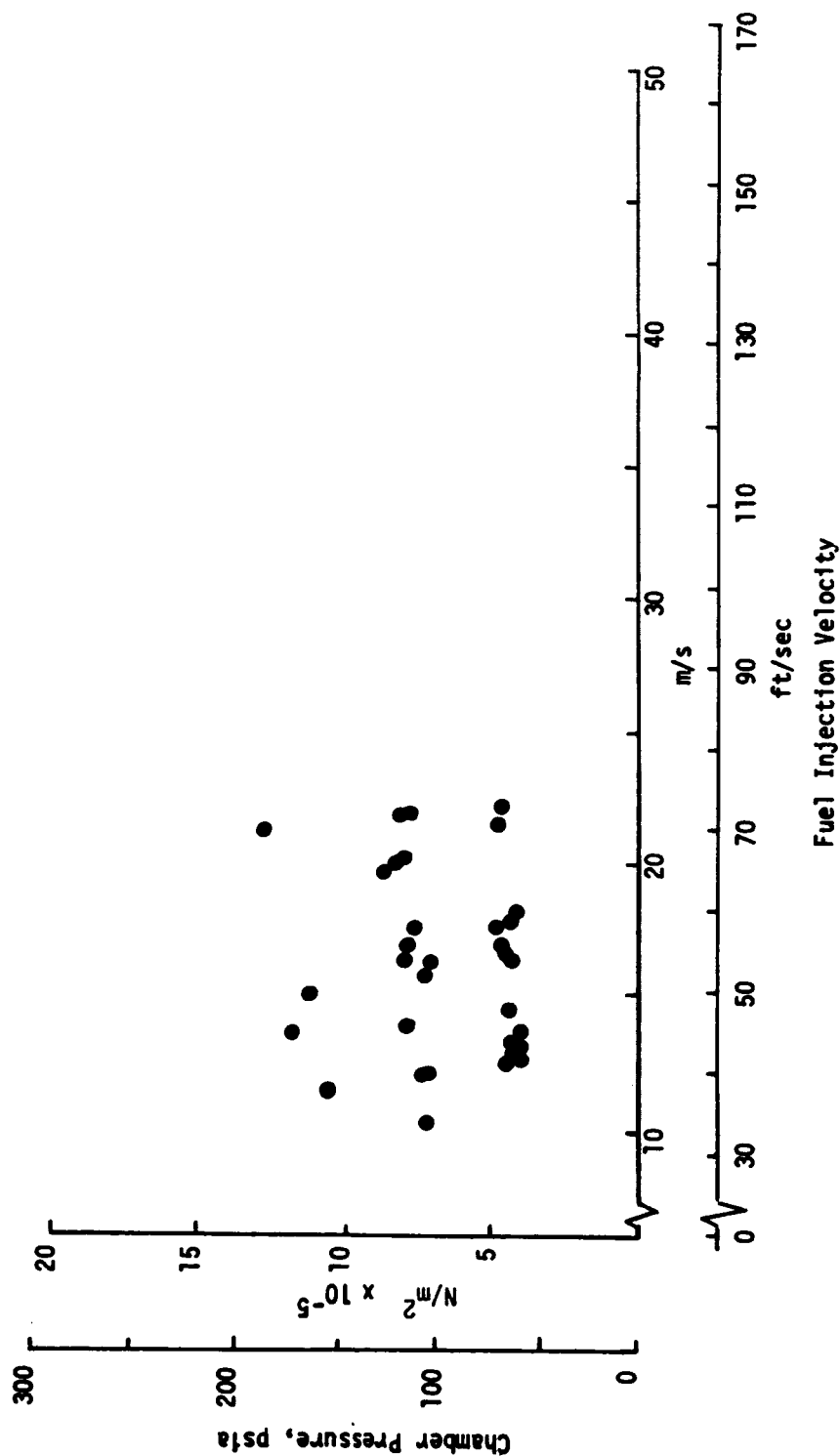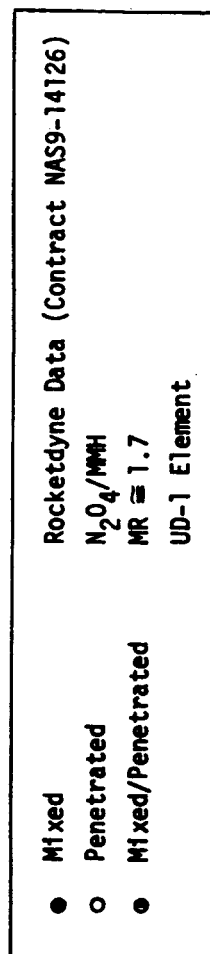   (113 psia)

   V_f - 30.2 m/s
        (99 ft/sec)

   t_f - 293°K (68°F)

B.   Penetrated Test Condition

Figure 5-1.   Typical Photographs of Mixed and
              Penetrated Test Conditions

Figure 5-2. Correlation of Fuel Injection Velocity and Chamber Pressure to Penetration for UD-1 Element
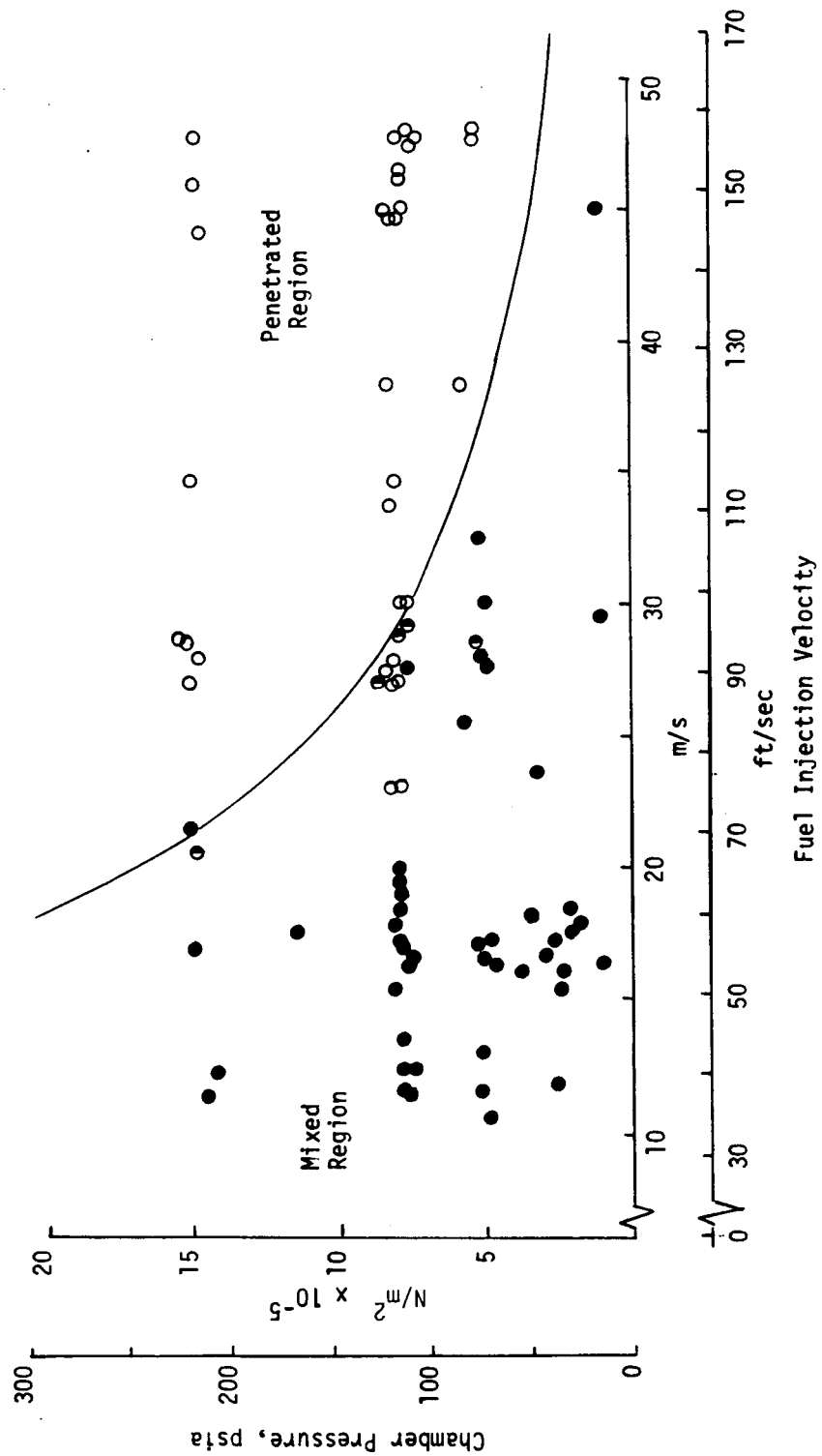
Figure 5-3.   Correlation of Fuel Injection Velocity and Chamber Pressure to
Penetration for UD-2 Element

Plots of chamber pressure versus fuel injection temperature are presented
in Figs. 5-4 and 5-5 for the UD-1 and UD-2 elements, respectively. Again,
no reactive stream separation was observed with the UD-1 element over the
range of parameters studied. Separation was observed with the UD-2 element
above ~322°K (120°F). Mixing occurs up to ~316°K (110°F). Note that only
tests with fuel injection velocities less than the value required for pene-
tration, are defined in Fig. 5-3, are plotted in Fig. 5-5. This was neces-
sary to avoid showing separated and/or penetrated conditions at low injection
temperatures that were due to high fuel injection velocity and not the fuel
injection temperature.

The results presented herein indicate that the orifice size, propellant
injection velocity, fuel temperature, and chamber pressure can signifi-
cantly effect reactive stream separation. Oxidizer injection temperature,
Rupe mixing index (ϕ), and mixture ratio were not varied over a sufficient
range to permit systematic cross plotting of their separate effects. How-
ever, there was no discernible effect of these latter variables on reactive
stream separation.

5.2 COLD FLOW EXPERIMENTS

Six cold (water) flow tests were conducted with the UD-1 and UD-2 elements
to verify that the doublet elements exhibit stable coherent jet character-
istics, good jet impingement, and well developed spray fans. The tests
were conducted over the same range of injection velocities and ϕ as the hot-
fire experiments. Test conditions are noted in Table 5-2.

Fastax motion pictures were taken at each test condition. Results of the
movies indicated that the elements exhibit stable coherent jet character-
istics, good jet impingement, and produce well developed spray fans with
non-reactive fluids.

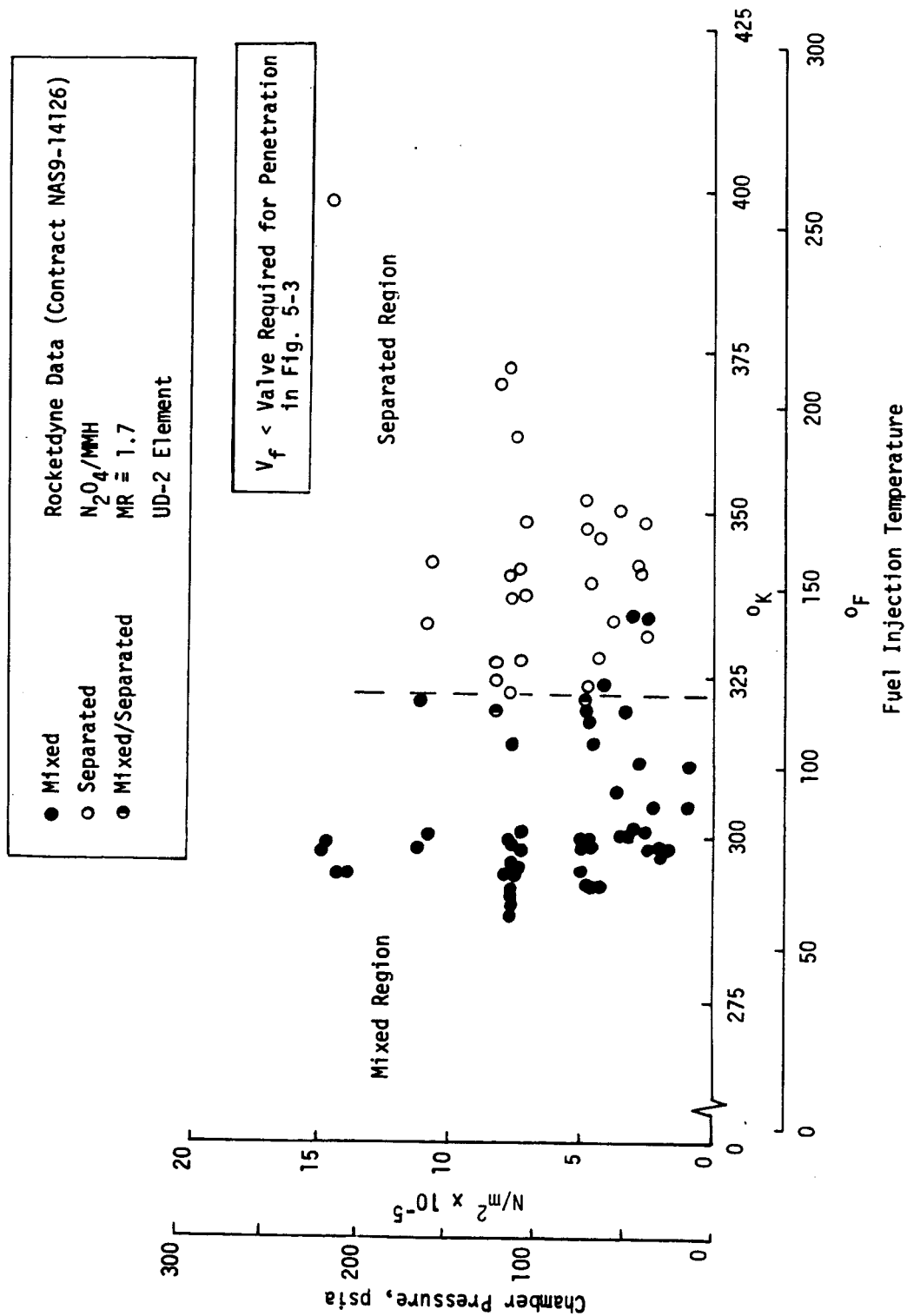Figure 5-4. Correlation of Fuel Injection Temperature and Chamber Pressure to Separation for UD-1 Element

Figure 5-5. Correlation of Fuel Injection Temperature and Chamber Pressure to Separation for UD-2 Element

6.0 DISCUSSION OF RESULTS

A discussion and correlation of the experimental results from this program (Contract NAS9-14126) and the concurrent related effort conducted by Aerojet (Contract NAS9-14186) are presented herein. Initially, the Aerojet study is briefly reviewed. The data from both programs are then correlated and design criteria are established which will allow for the design of stable high performing injectors that are free from reactive stream separation.

6.1 REVIEW OF RELATED CONTRACT NAS9-14186 STUDY

Concurrent with the investigation conducted by Rocketdyne, Aerojet Liquid Rocket Company conducted a related effort NASA Contract NAS9-14186 (Ref. 27). Applicable data from that contract are presented as Appendix A.

Aerojet conducted approximately 90 tests employing N_2O_4/MMH with an element similar in design to the UD-1 element employed in this study. During that investigation, chamber pressure was varied from an absolute pressure of 5.4 to 68 atm (80 to 1000 psia), fuel injection temperature from 277 to 422 ^{O}K (40 to 300°F), oxidizer injection temperature from 283 to 338°K (50 to 150°F), and propellant injection velocities from ~9 to 55 m/sec (30 to 180 ft/sec). Nominal mixture ratio for all was ~1.7. Consequently, in addition to conducting tests over the same range of test conditions as on this contract, Aerojet conducted tests at higher injection velocities, chamber pressure, and fuel temperature with the UD-1 element.

Several important differences in the experimental test setup and/or data interpretation between this study and Aerojets' should be noted. Whereas Rocketdyne employed only backlighting of the spray field, Aerojet utilized one lamp to backlight the spray area and with second and third lamps provided top and front lighting. Rocketdyne employed only backlighting because previous experience (Refs. 11, 13, and 21) had indicated that this

was the most effective means of lighting for definition of mixed versus separated/penetrated test conditions. Separation/penetration being defined as a clearly defined separation of the spray fan downstream of the jet impingement point. Aerojet (Ref. 27) on the other hand, appears to define separation and/or penetration as the appearance of unmixed propellants in the spray field evidenced by color differences between the fuel and oxidizer. Energetic cyclic blowapart (i.e., popping) was not observed on any of the tests conducted by Aerojet or Rocketdyne.

6.2 DATA CORRELATION

Two different types of reactive stream separation, with different driving mechanisms, appear to have been observed during the conduct of the subject contracts. One of these occurs at high injection velocities and/or chamber pressure with ambient temperature or moderately heated propellants. The other, occurs at elevated propellant (fuel) temperatures. Development of models to predict test conditions which will not result in the occurrence of reactive stream separation by either of the two phenomenon are presented in the following paragraphs. These models can be employed as guidelines in the design of stable, high performing injectors free from reactive stream separation.

6.2.1 Impinging Jet Characteristics Model

A model, termed Impinging Jet Characteristics Model, to characterize the ambient temperature or moderately heated propellants reactive stream separation phenomena, was developed based on Rocketdyne's data on the UD-1 and UD-2 elements and Aerojet's UD-1 element data. As was noted in Section 5.0, Rocketdyne observed what it termed "penetration" at the higher injection velocities and chamber pressures with the UD-2 element. Similarly, Aerojet observed what it called "separation" at the higher injection velocities and chamber pressures with the UD-1 element.

Plots of chamber pressure versus fuel injection velocity for the UD-1
and UD-2 elements are presented as Figs. 6-1 and 6-2, respectively. A
distinction as to whether each test was mixed, separated, penetrated,
etc., is made in the figures. In addition, a differentiation between
Rocketdyne and Aerojet data is made in Fig. 6-1. With the exception
of whether the UD-1 element is mixed or penetrated at low injection
velocities, Rocketdyne's and Aerojet's data are consistent (Fig. 6-1).
The similarity between the data plots for the UD-1 and UD-2 elements
should be noted. Both predict reactive stream separation at the higher
injection velocities in combination with higher chamber pressures.
Rocketdyne called the phenomena penetration (Fig. 6-2), while Aerojet
termed it separation; however, both agree that some form of reactive
stream separation occurs at the higher injection velocities in combina-
tion with higher chamber pressures. Separated, penetrated, and mixed
regions are noted on the figures. Reactive stream separation occurs at
lower injection velocities and chamber pressures with the larger element
(UD-2).

It should be noted that only tests conducted with fuel injection temperatures
less than the value required for separation due to fuel temperature effects
($T_f < 338^{\circ}$K for the UD-1 element and less than 316°K for the UD-2 element)
are shown in Figs. 6-1 and 6-2. Definition of these temperature limits is
established later. This was necessary to avoid the confusion of showing
separated conditions at low injection velocity that were due to fuel tem-
perature effects and not injection velocity effects.

As was initially suggested by Aerojet (Ref. 27), the penetration/separation
which occurs at higher injection velocities and chamber pressures can be
related to the Weber number of the impinging jets. This is illustrated in
Figs. 6-3 and 6-4 in which chamber pressure is plotted versus the fuel stream
Weber number for the UD-1 (Fig. 6-3) and UD-2 (Fig. 6-4) elements. Both
Rocketdyne and Aerojet data are presented in these figures. As was the case
in Figures 6-1 and 6-2, the Rocketdyne and Aerojet data are consistent with
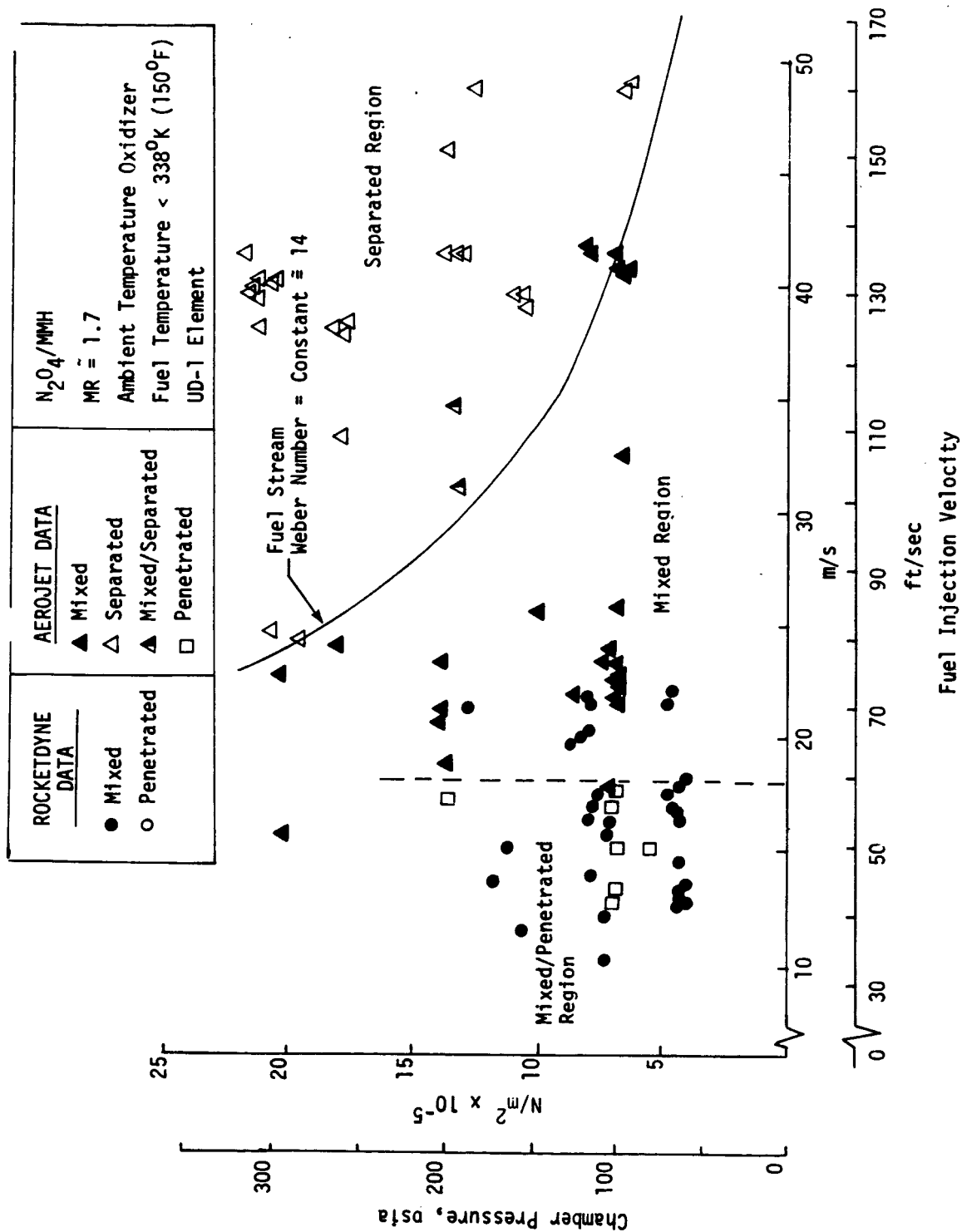
Figure 6-1. Correlation of Reactive Stream Separation to Chamber Pressure and Fuel Injection Velocity for UD-1 Element
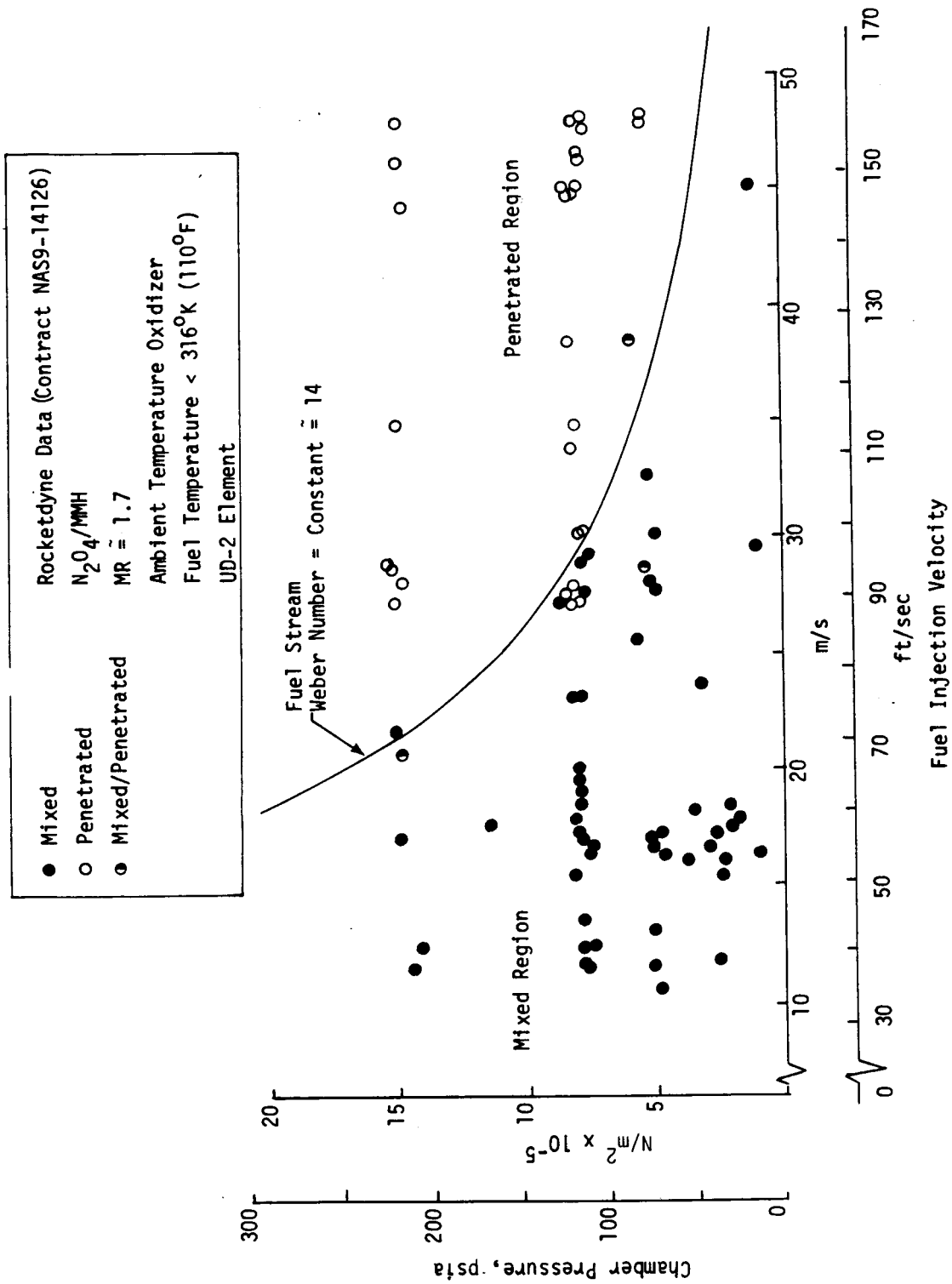
Figure 6-2. Correlation of Reactive Stream Separation to Chamber Pressure and Fuel Injection Velocity for UD-2 Element
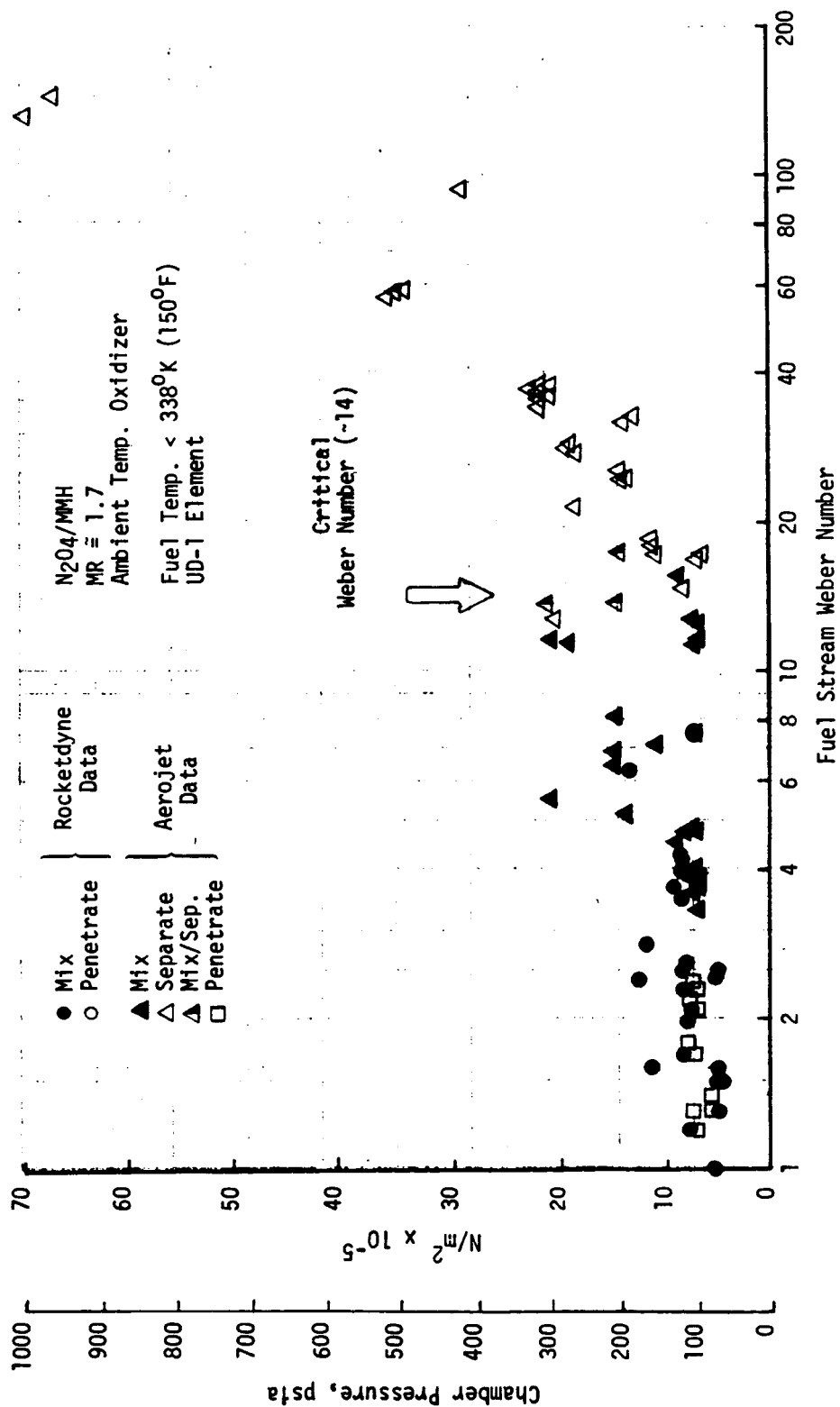
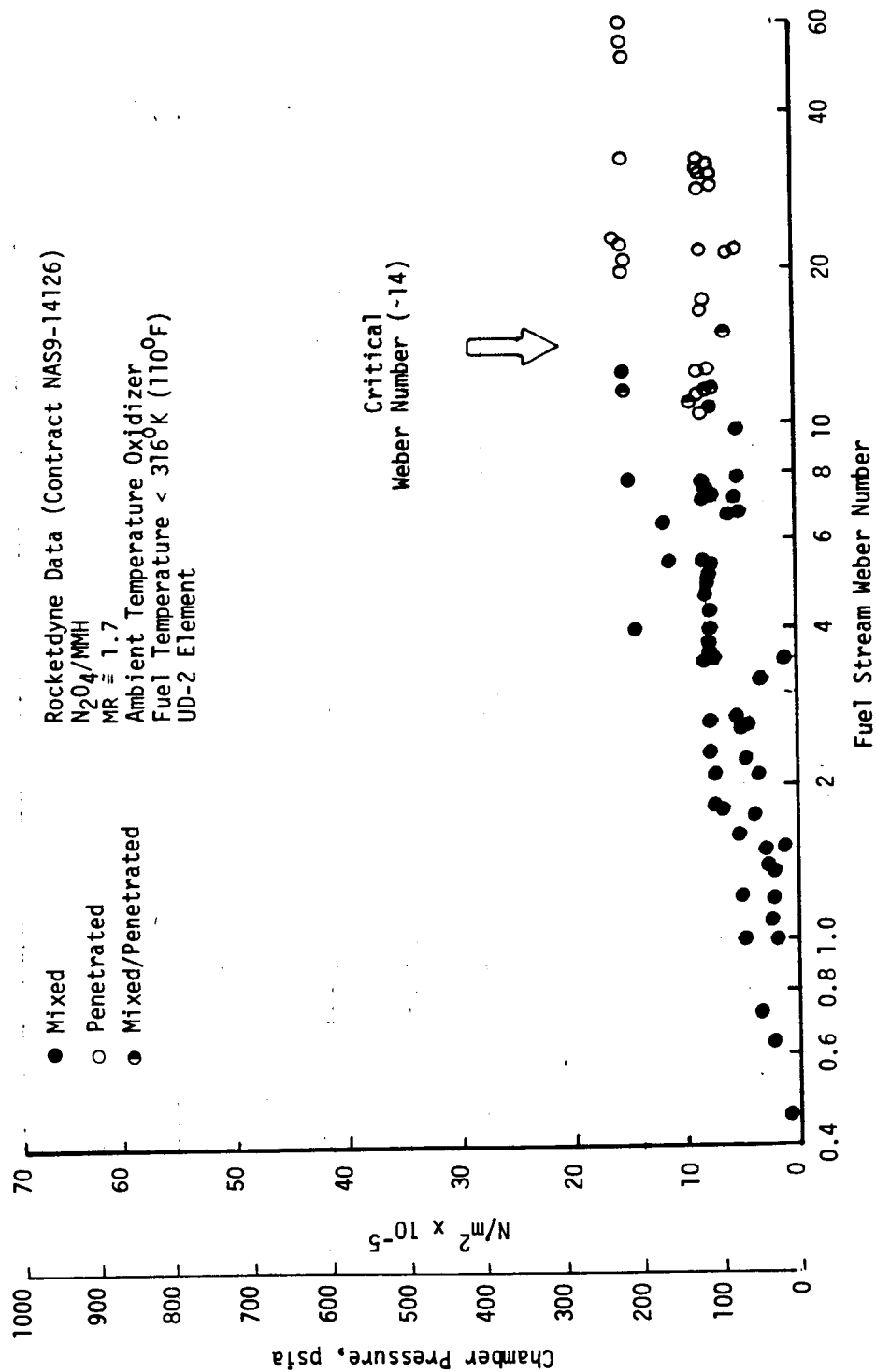Figure 6-3. Correlation of Reactive Stream Separation to Fuel Stream Weber Number for UD-1 Element

Figure 6-4. Correlation of Reactive Stream Separation to Fuel Stream
Weber Number for UD-2 Element

the possible exception of whether the UD-1 element is mixed or penetrated at low injection velocities/Weber numbers. Reactive stream separation occurs above a critical Weber number of ~14 for both elements. Curves of constant fuel stream Weber number are shown in Figs. 6-1 and 6-2.

The Weber numbers shown plotted in Figs. 6-3 and 6-4 were calculated as follows:

$$\text{Weber No.} = \frac{\rho_g \, v_f^2 \, d_f}{\sigma_f \, g_c} \qquad (6-1)$$

where

ρ_g = combustion gas density

v_f = fuel injection velocity

d_f = fuel orifice diameter

σ_f = surface tension of the fuel

g_c = gravitational constant $\left(32.174 \, \frac{lbm}{lbf} \cdot \frac{ft}{sec^2}\right)$

The gas density employed in the calculation of the Weber number was the combustion gas density at the injected mixture ratio. The Weber number is a ratio of aerodynamic-to-surface-tension forces for the jet.

The above correlation of data does not apply to tests conducted with fuel injection temperatures above the critical values noted in Figs. 6-1 and 6-2. That is, above fuel temperatures of 338^oK (150^oF) for the UD-1 element and 316^oK (110^oF) for the UD-2 element. Separation will occur above these temperatures for reasons to be explained later. Tests conducted with fuel temperatures above these critical values can exhibit separation at low Weber numbers (i.e., at Weber numbers <14).

As noted above, the phenomena observed at high injection velocites and chamber pressures with ambient temperature or moderately heated fuel was termed "penetration" by Rocketdyne and "separation" by Aerojet. The cause of the phenomena is not clear; however, several mechanisms have been proposed.

6-8

Aerojet (Ref. 27) has suggested that it may be due to high shear forces on the surface of the jet which causes some degree of self atomization, increased interfacial area and surface reactions and, thereby, separation. On the other hand, it may be due to the relative stability of the jets at high velocity.

A generalized correlation of the data for the UD-1 and UD-2 elements is presented in Fig. 6-5. Chamber pressure is shown plotted as a function of fuel injection velocity in this figure. Regions of mixing and reactive stream separation are noted. Note that the smaller element is less sensitive to chamber pressure and injection velocity effects (i.e., it is free from reactive stream separation over a greater range of P_c, v_f, and T_f).

It should be noted that since most of the tests were conducted at a nominal mixture ratio of ~1.7, a similar correlation could have been developed based on the oxidizer stream Weber number. Values of the oxidizer stream Weber number were approximately the same as for those of the fuel stream.

6.2.2 Heated Propellant Model

A heated propellant reactive stream separation model was developed based on both Rocketdyne's and Aerojet's data. As was noted in Section 5, the reactive stream separation phenomena occurring with heated propellants (termed separation) appeared to be different than the penetration phenomena observed at high injection velocities and chamber pressures with ambient temperature or moderately heated propellants.

Plots of chamber pressure versus fuel injection temperature for the UD-1 and UD-2 elements are presented as Figs. 6-6 and 6-7, respectively. A distinction as to whether each test is mixed, separated, or mixed/separated is made in the figures. Differentiation between Rocketdyne and Aerojet data is also made in Fig. 6-6. Tests with fuel stream Weber numbers greater than the critical value of ~14 and the low velocity penetrated tests reported by

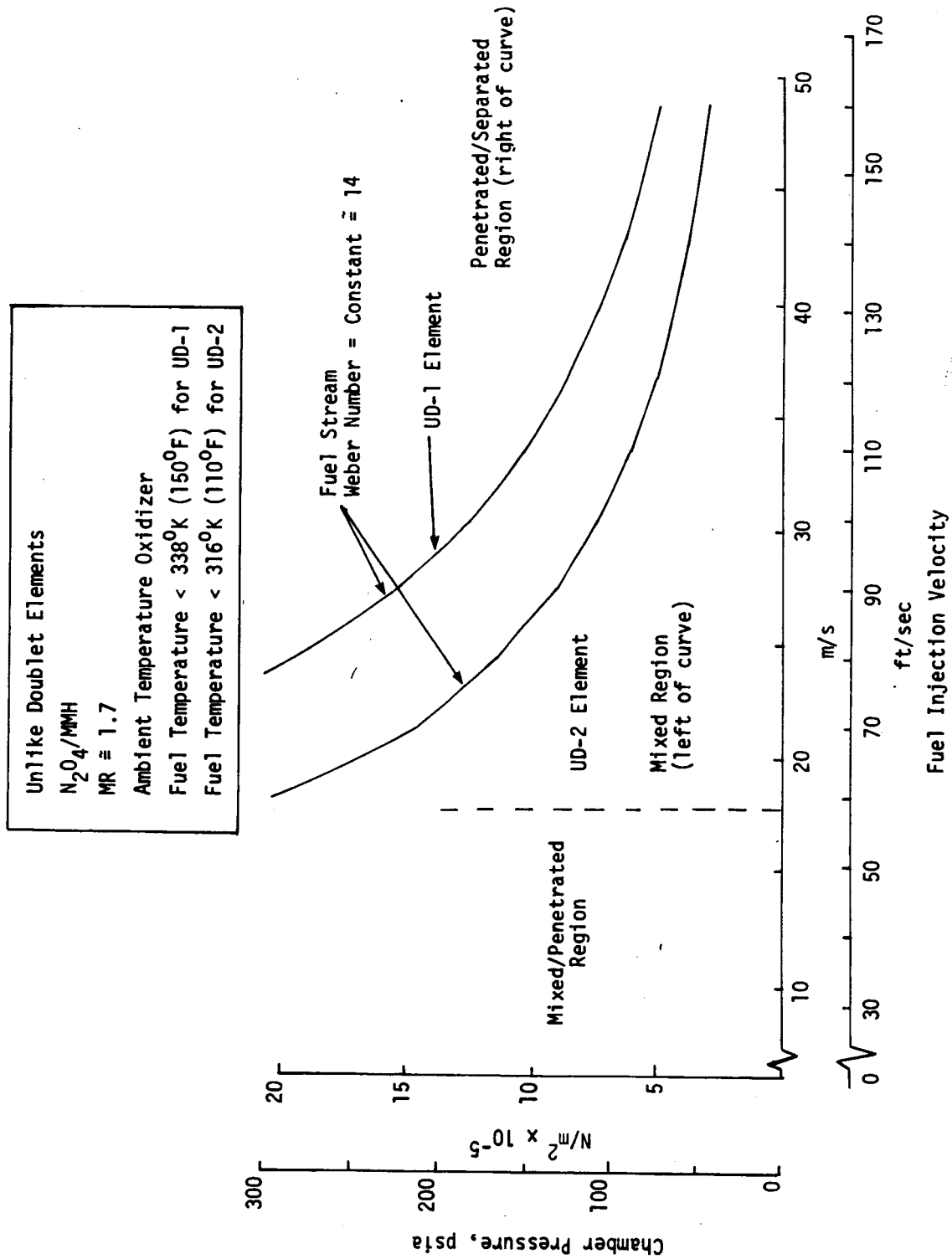Figure 6-5. Generalized Correlation of Reactive Stream Separation to Chamber Pressure and Injection Velocity for Unlike Doublet Elements
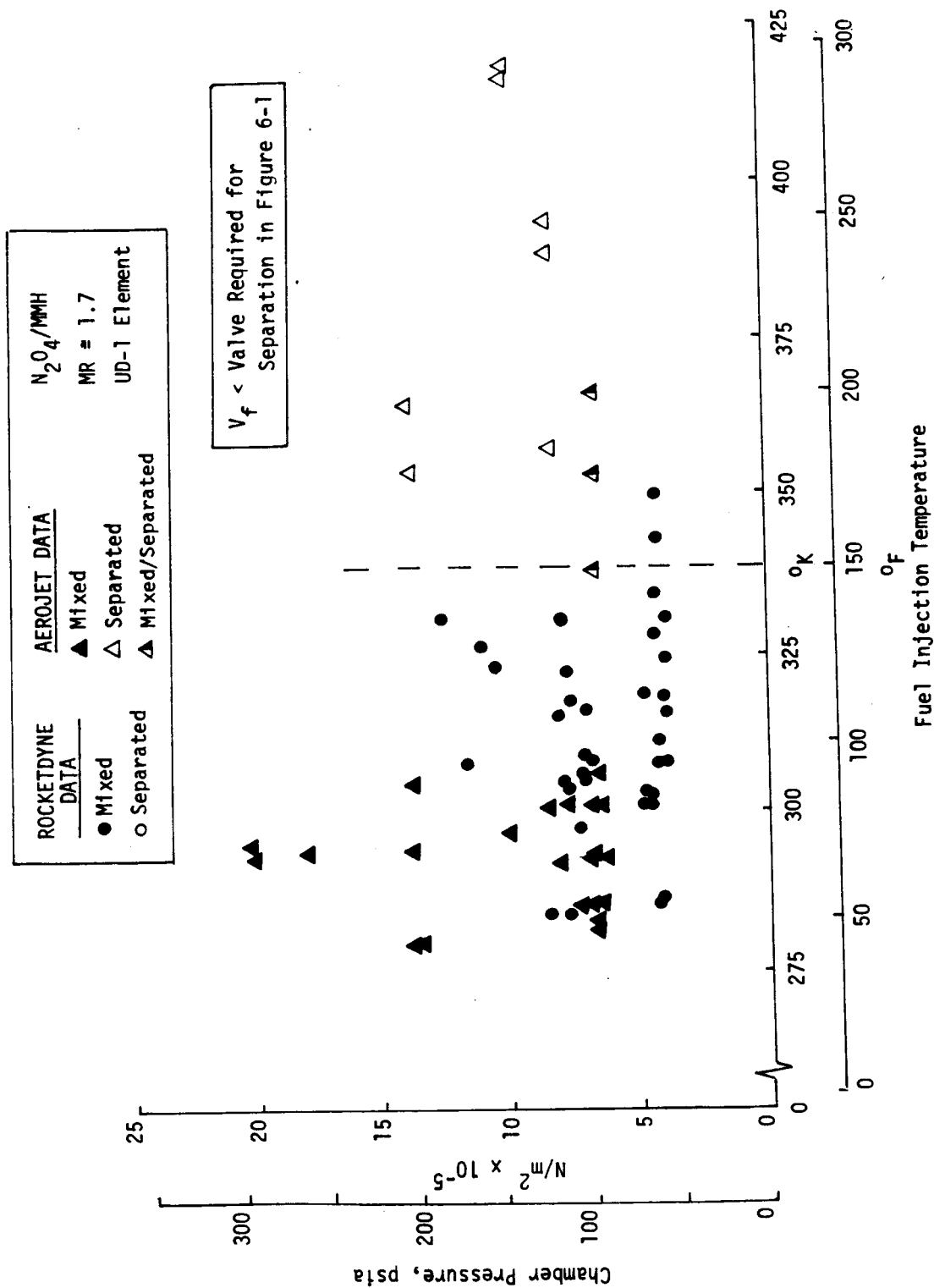
Figure 6-6.   Correlation of Reactive Stream Separation to Chamber Pressure and
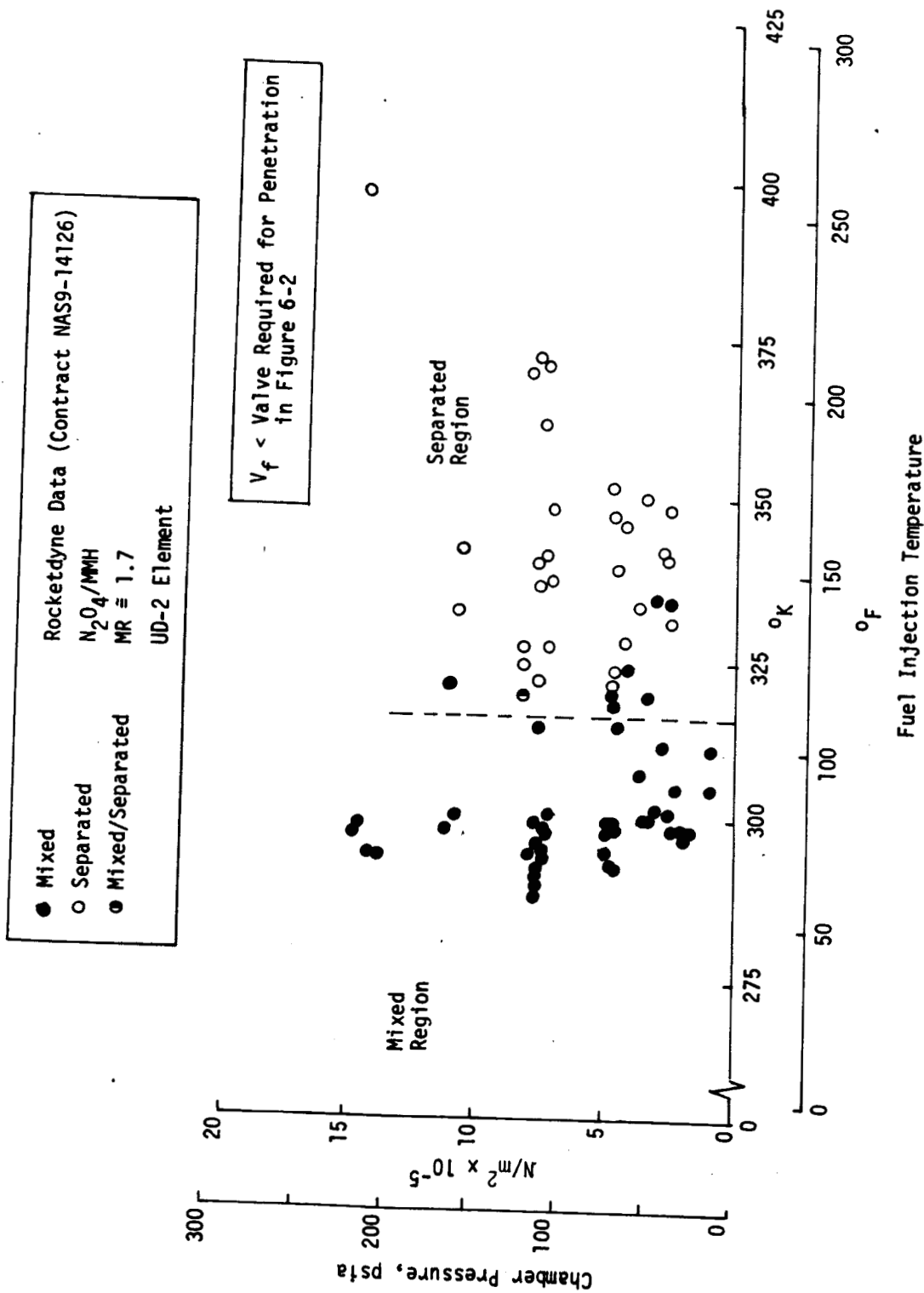   Fuel Injection Temperature for UD-1 Element

Figure 6-7. Correlation of Reactive Stream Separation to Chamber Pressure and Fuel Injection Temperature for UD-2 Element

Aerojet are not included on these plots. These data would only add confution to the analysis of fuel temperature effects on separation. The effect of fuel injection temperature on separation is quite evident. As would be expected from the method of data analysis (i.e., the method of defining tests as mixed, separated, or mixed/separated), which is qualitative and subjective, a clear cut maximum temperature without separation is not evident. However, it appears that in general separation occurs at fuel temperatures above ~338°K (150°F) with the UD-1 element and above ~316°K (110°F) with the UD-2 element. The larger element (i.e., the element with the larger orifice diameters) is more sensitive to the fuel injection temperature.

It should be noted that the data in Figs. 6-6/6-7 suggest that there may be an interaction of effects (chamber pressure and fuel temperature) on separation. The data suggests that it may be possible to operate at a higher fuel injection temperature at lower chamber pressures without separation.

6.2.2.1 Derivation of Theoretical Model. A theoretical model was developed to provide a more systematic basis for correlation of the heated fuel experimental reactive stream separation data to significant parameters. Formulation of this model was anticipated to provide insight into the significant parameters affecting separation and in turn lead to suggestions for the development of a better analytical model. Because available data indicate that energetic cyclic separation (popping) does not occur with the N_2O_4/MMH system over the range of element sizes investigated, the model does not provide for its description; however, addition

of this capability to a more generalized model can be made if warranted by future experimental results.

The theoretical model assumes that reactive stream separation occurs primarily thorugh the gas evolution resulting from a chemical reaction equivalent to that shown in Eq. (6-2).

$$CH_3NHNH_2 + N_2O_4 \rightarrow 2\ N_2 + 3\ H_2O + CO \tag{6-2}$$

The heat of reaction for process shown by Eq. (6-2) is approximately 7500 Btu/lbm of MMH reacted or approximately 5.7×10^4 Btu/lb mole of product gas formed. The reaction is assumed to occur very rapidly in a mixing zone within the doublet spray fan as shown in Fig. 6-8. The mixing zone originates at the jet impingement point and is assumed to grow linearly with downstream distance from this point until it completely fills the liquid sheet. The overall length of the sheet is L_c, the downstream distance at which it breaks up into droplets and ligaments. Intimate mixing of both mass and energy are assumed within the mixing zone, i.e., the heat from reaction is assumed to be absorbed principally by the unreacted liquids in the mixing zone and the product gas is in thermal equilibrium with the liquid.

The generation of blowapart-producing gas is assumed to follow a zero order reaction mechanism defined by the Arrhenius relation

$$\frac{d\ V_g}{dt} = \mathcal{R} = Ae^{-\Delta E/R_g T} \tag{6-3}$$

where V_g is the volume of gas generated per unit volume of mixed reaction zone, A is the zero order reaction rate constant ($time^{-1}$) and the remaining symbols have their usual meaning as defined in the Nomenclature section. With the usual transformation for flow problems

$$dt = \frac{1}{U}\ dx \tag{6-4}$$

6-14
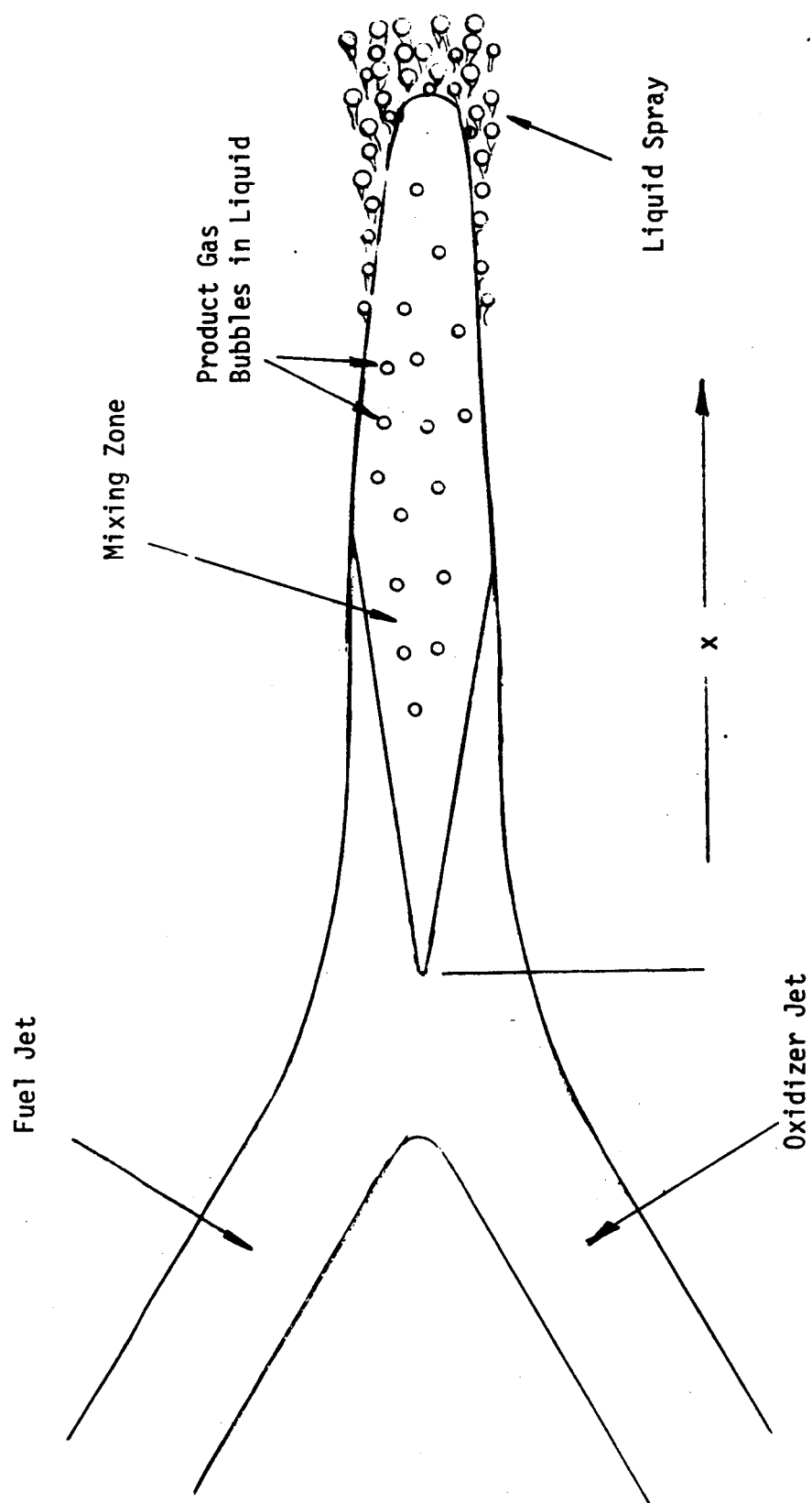
Figure 6-8. Doublet Sheet Model for Theoretical Analysis of Separation

Eq. (6-3) becomes

$$\frac{d\,V_g}{dx} = \frac{A}{U}\,e^{-\Delta E/R_g T} \tag{6-5}$$

The volumetric rate of heat generation is given by

$$\frac{dQ}{dt} = \rho_g\,\mathcal{R}\Delta H \tag{6-6}$$

Combining Eqs. (6-4), (6-5), and (6-6) gives

$$\frac{dQ}{dx} = \Delta H\,\rho_g\,\frac{Ae^{-\Delta E/R_g T}}{U} = \Delta H\,\rho_g\,\frac{\mathcal{R}}{U} \tag{6-7}$$

If the heat generated by the reaction is assumed to be absorbed by the liquid in the mixing zone with a resultant temperature rise, the temperature rise will, in turn, increase the reaction rate. Differentiating Eq. (6-3) with respect to temperature and then with respect to distance along the liquid sheet

$$\frac{d\mathcal{R}}{dT} = Ae^{-\Delta E/R_g T}\left(\frac{\Delta E}{R_g T^2}\right) = \mathcal{R}\left(\frac{\Delta E}{R_g}\right)\frac{1}{T^2}$$

$$\frac{d\mathcal{R}}{dx} = \frac{d\mathcal{R}}{dT}\,\frac{dT}{dx} = \left(\frac{\Delta E}{R_g T^2}\right)\mathcal{R}\,\frac{dT}{dx} \tag{6-8}$$

The analysis presented in Appendix C indicates that the total reaction required to produce a blowapart condition is a very small fraction of the total flow. This also indicates that the temperature rise in the mixed reaction zone can be assumed to be a small fraction of the absolute temperature which can be approximated by a mean temperature in the term $(\Delta E/R_g T^2)$. Defining

$$K_1 = \Delta E / R_g \bar{T}^2 \cong \Delta E / R_g \, T_0^2$$

$$\frac{d\mathcal{R}}{dx} = K_1 \mathcal{R} \, \frac{dT}{dx} \tag{6-9}$$

But

$$\frac{dT}{dx} = \frac{1}{C_p \, \rho_L} \frac{dQ}{dx} = \frac{\Delta H}{C_p} \left(\frac{\rho_g}{\rho_L}\right) \frac{\mathcal{R}}{U} \tag{6-10}$$

Combining Eq. (6-9) and (6-10), and re-arranging

$$\frac{d\mathcal{R}}{\mathcal{R}^2} = \frac{\Delta H}{C_p} \left(\frac{\rho_g}{\rho_L}\right) \frac{K_1}{U} \, dx \tag{6-11}$$

Integrating and re-arranging

$$\mathcal{R} = \frac{\mathcal{R}_0}{1 - \frac{\Delta H}{C_p \, T_0^2} \left(\frac{\rho_g}{\rho_L}\right)\left(\frac{\Delta E}{R_g}\right)\left(\frac{x}{U}\right) \mathcal{R}_0} \tag{6-12}$$

By assuming the generated gas in the reaction zone to be in thermal equilibrium with the liquid, which is in turn close to the impingement point temperature T_0, the gas density can be approximated by

$$\rho_g = \frac{P}{R_g \, T_0}$$

Therefore,

$$\mathcal{R} = \frac{\mathcal{R}_0}{1 - \frac{\Delta H}{C_p \, T_0^3} \left(\frac{P}{\rho_L}\right) \frac{\Delta E}{R_g^2} \left(\frac{x}{U}\right) \mathcal{R}_0} \tag{6-13}$$

The functional relation between gas generation rate $\mathcal{R}$ and x shown in Eq. (6-13) defines a critical distance x_c at which the gas generation reaches a critical value $\mathcal{R}_c$. Re-arranging Eq. (6-13) to solve for x_c gives

$$x_c = \frac{U\, T_0^{\,3}}{\left(\frac{\Delta H}{C_p}\right)\left(\frac{P}{\rho_L}\right)\left(\frac{\Delta E}{R_g^{\,2}}\right)\mathcal{R}_c}\left[\frac{\mathcal{R}_c}{\mathcal{R}_0} - 1\right]$$

To develop a useful correlation, the critical reaction length x_c is divided by a critical hydrodynamic length L_c, defined as being the point at which the spray fan has spread sufficiently that blowapart cannot occur. The most obvious choice for L_c is the ligament length (i.e., the distance downstream of the impingement point at which the liquid breaks up into droplets and ligaments). This distance is defined by

$$L_{C_1} = C_1 \frac{D}{U} \tag{6-14}$$

where C_1 has a value of 61 m/sec (200 ft/sec) for water jets of equal diameter (Ref. 9). However, photographic studies conducted at Rocketdyne have indicated that for injection velocities and orifice diameters similar to those of this study this distance is approximately one jet diameter, i.e.,

$$L_{C_2} = D \tag{6-15}$$

It may, however, be that the mixing length which has been observed to be proportional to the jet diameter, i.e.,

$$L_{C_3} = C_3 D \tag{6-16}$$

where $C_3 \cong 2$ (Ref. 9) should be employed.

Development of equations and attempts to correlate the data were carried out using each of the above equations to define L_C. In general, data for either element could be correlated well by substitution of an expression for L_C that was proportional to the jet diameter (i.e., Equations 6-15/6-16) into Eq. (6-13). However, to collapse the data for both elements to a single correlation it was necessary to consider L_C as a constant. Considering the size of the elements and range of injection velocities studied, this assumption does not seem illogical. A value for L_C equal to the mean diameter of the elements orifices was employed in the final correlation of the data, i.e.,

$$L_{C_4} = 0.07430 \text{ cm } (0.02925\text{-inch}) = C_4 \tag{6-17}$$

Development of the equation used to correlate the data will be carried out using Eq. (6-17) to define L_C. Equation (6-13) becomes

$$\frac{x_C}{L_C} = \frac{U T_0^3}{C_4 P \left(\frac{\Delta H}{C_p \rho_L}\right)\left(\frac{\Delta E}{R_g^2}\right) \mathcal{R}_C} \left[\frac{\mathcal{R}_C}{\mathcal{R}_0} - 1\right] \tag{6-18}$$

Equation (6-18) can be divided into dimensionless groups as follows:

$$\left(\frac{x_C}{L_C}\right) = \left[\frac{U T_0^2 C_p \rho_L R_g}{C_4 P \Delta H \mathcal{R}_C}\right]\left(\frac{R_C T_0}{\Delta E}\right)\left[\frac{\mathcal{R}_C}{\mathcal{R}_0} - 1\right] \tag{6-19}$$

The critical reaction rate $\mathcal{R}_C$ (volume/volume time) is expected to be proportional to the velocity, U, i.e.,

$$\mathcal{R}_C = BU \tag{6-20}$$

Equation (6-19) becomes

$$\left(\frac{x_c}{L_c}\right) = \left[\frac{T_o^2 \, C_p \, \rho_L \, R_g}{C_4 \, B \, P \, \Delta H}\right] \left(\frac{R_g \, T_o}{\Delta E}\right) \left[\frac{BU}{\text{o}} - 1\right] \tag{6-21}$$

with

$$\mathcal{R}_o = Ae^{-\Delta E/R_g \, T_o} \tag{6-22}$$

Mixing occurs when (x_c/L_c) is greater than unity. Separation is predicted to occur for (x_c/L_c) less than unity. Evaluation of required constants B, A, and ΔE must be made by correlation of appropriate experimental data.

6.2.2.2 Model Correlation.

Although Eq. (6-21) is in non-dimensional form, it contains dimensional coefficients B, ΔE and A which are dimensional and are initially unknown. To correlate the experimental data to the model, Eq. (6-21) is first re-arranged as follows:

$$\left(\frac{x_c}{L_c}\right) \left[\frac{T_o^3 \, C_p \, \rho_L \, R_g^2}{C_4 \, P \, \Delta H}\right]^{-1} = \left(\frac{1}{B\Delta E}\right) \left[\frac{BU}{A} e^{\Delta E/R_g \, T_o} - 1\right] \tag{6-23}$$

so that the known and unknown parameters have been separated into new non-dimensional groups. It can now be noted that when

$$\frac{BU}{A} e^{\Delta E/R_g \, T_o} \leq 1$$

the doublet must be separated because the reaction rate at the impingement point is already greater than the critical rate. The operating regime of interest (particularly for purposes of correlation) occurs when

$$\frac{BU}{A} e^{\Delta E/R_g \, T_o} - 1 \sim \frac{BU}{A} e^{\Delta E/R_g \, T_o}$$

In this case, Eq. (6-23) becomes

$$\left(\frac{x_c}{L_c}\right)\left[\frac{U\,T_o^{\,3}\,C_p\,\rho_L\,R_g^{\,2}}{C_4\,P\,\Delta H}\right]^{-1} = \frac{1}{\Delta E A}\,e^{\Delta E/R_g\,T_o} \tag{6-24}$$

Although the value of (x_c/L_c) during a given hot firing experiment is unknown, it is known that

$x_c/L_c < 1$ gives separation

$x_c/L_c > 1$ gives mixing

$x_c/L_c = 1$ is the boundary between separation and mixing

Rocketdyne's hot firing data with the UD-1 and UD-2 elements together with the data of Aerojet with the UD-1 element were correlated by plotting

$$\left[\frac{U\,T_o^{\,3}\,C_p\,\rho_L\,R_g^{\,2}}{C_4\,P\,\Delta H}\right]^{-1} \qquad \text{versus } 1/T_o$$

on semilog paper with

$C_4 = 0.02925\text{-inch}$

$U = v_f$

$$P = P_c + \frac{\rho_L\,v_f^{\,2}}{2g}$$

$T_o = T_{Inj}$ of the hotter propellant

It should be noted that as long as ϕ is near unity the effect of using v_f for U will be compensated by a change in the eventual definitions of B and A. The results of the correlations are presented in Fig. 6-9. Aerojet's low velocity penetration tests and those tests for which reactive stream separation is indicated by the Impinging Jet Characteristics Model are not included in the data correlation. The plot shows a reasonable correlation of the data in view of the qualitative and subjective means of determining mixed versus separated test conditions.

If the boundary between the separated and mixed regions is assumed to be that shown by the line in Fig. 6-9, then the slope of the line defines a value for the activation energy ΔE of 13.0×10^6 ft lb/lb mole. With this value of ΔE, a value of 1.7×10^{10} sec^{-1} was calculated for the frequency factor A. It is important to note that these values are reasonable for these propellants.

With values of ΔE and A defined, Eq. (6-24) can be rearranged as follows to provide a design criteria to prevent separation. That is,

$$\frac{x_c}{L_c} = \frac{1}{\Delta E A} e^{\Delta E / R_g T_o} \left[\frac{U T_o^3 C_p \rho_\ell R_g^2}{C_4 P \Delta H} \right] > 1 \qquad (6\text{-}25)$$

The value of all quantities required to calculate $\frac{x_c}{L_c}$ are known.

It is believed that the correlation of data obtained with the above model provides insight into the significant parameters affecting separation and can in turn lead to suggestions for the development of a better analytical model.
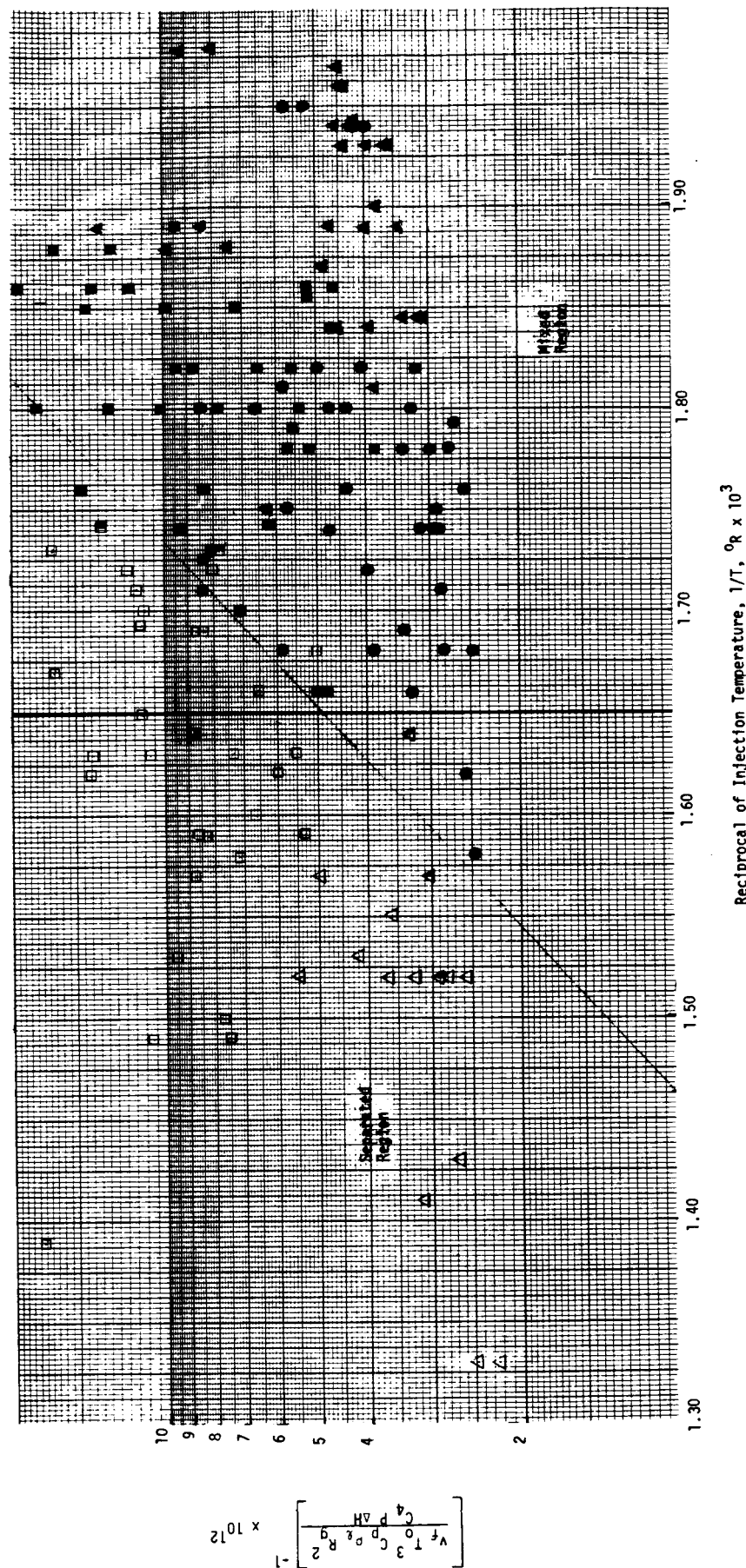
Figure 6-9. Correlation of Experimental Data According to Model of Equation (6-24)

6.3 DESIGN CRITERIA

The data correlations presented in the previous section of this report (Section 6.2) provide design criteria (guidelines) which will allow for the design of stable high performing injectors that are free from reactive stream separation. Since two different types of reactive stream separation, with different driving mechanisms, were observed, two reactive stream models were developed. Each of the models define a design criteria that should be employed in the design of an injector to ensure that it is free from reactive stream separation.

To prevent penetration, the design criteria established by the Impinging Jet Characteristics Model (Section 6.2.1) should be employed. That is, the injector should be designed with

$$\text{Weber Number} = \frac{\rho_g \, v_f^2 \, d_f}{\sigma_f \, g_c} < 14 \qquad (6\text{-}26)$$

To prevent separation which can occur with heated propellants, the design criteria established from the Heated Propellant Model (Section 6.2.2) should be employed. That is, the injector should be designed according to the following criteria.

$$\frac{x_c}{L_c} = \frac{1}{\Delta EA} e^{\Delta E/R_g T} \left[\frac{v_f \, T_o^3 \, C_p \, \rho_\ell \, R_g^2}{C_4 \, P \, \Delta H} \right]$$

where

$$\frac{x_c}{L_c} < 1 \quad \text{gives separation}$$

$$\boxed{\frac{x_c}{L} > 1 \quad \text{gives mixing}}$$

$$\frac{x_c}{L_c} = 1 \quad \text{is the boundary between separation and mixing}$$

where

$$\Delta E = 13.0 \times 10^6 \text{ ft lb/lb mole}$$

$$A = 1.7 \times 10^{10} \text{ sec}^{-1}$$

$$C_4 = 0.02925\text{-inch}$$

The value of all quantities required to calculate $\frac{x_c}{L_c}$ are known.

7.0 CONCLUDING REMARKS AND RECOMMENDATIONS

The objectives of this study were: (1) to develop an understanding of the mechanisms that cause reactive stream separation for hypergolic propellants, and (2) through a basic understanding of the governing mechanisms, establish design criteria which would allow for the design of stable high performing injectors that are free from reactive stream separation. These objectives were achieved.

The investigation was limited to the N_2O_4/MMH propellant combination, unlike-doublet-type element, and to a range of operating conditions applicable to the Space Tug and Space Shuttle attitude control and maneuvering engines. Use of the design criteria established herein for other propellant combinations or element types is not recommended; however, the experimental technique employed and basic understanding of the phenomenon occurring could be applied to establish design criteria for other propellant combinations and/or other element types.

From the experimental data obtained it was concluded that two different types of reactive stream separation, with different driving mechanisms, were observed. One of these, termed penetration, was observed at high injection velocities and/or chamber pressures with ambient temperature or moderately heated (fuel) propellants. The other phenomena, termed separation, occurred at elevated fuel temperatures. In both cases, the observed reactive stream separation phenomenon consisted of repeated pulses (i.e., it was cyclic). However, the pulsing did not exhibit the strength necessary to either disrupt the doublet jets upstream of the impingement point or to completely destroy the spray fan downstream of the impingement point; i.e., there were no instances of energetic stream blowapart or "popping" observable in the film data. The frequency of the cycle phenomenon was on the order of 10 to 20 cycles per second.

It is further concluded that the tendency toward reactive stream separation increases with increasing fuel injection temperature, element orifice size,

chamber pressure, and propellant injection velocity. The results
of this investigation suggest that if an unlike-doublet element
injector is employed for the application investigated (i.e., Space
Tug and Space Shuttle attitude control and orbital maneuvering engines)
small element orifice diameters and/or moderate fuel injection
temperatures will be required to ensure operation in a regime without
reactive stream separation.

Specifically, the following recommendations for future effort are:

1. Investigate the use of other element types such as
    like doublets and/or triplets.

2. Study other propellant combinations such as N_2O_4/50-50
    and/or ClF_3/MMH.

3. Conduct further studies with the unlike-doublet element
    and investigate more thoroughly the effects of orifice
    size and jet stability characteristics.

If further studies of this nature are conducted, serious consideration
should be given to the possible use of a more quantitative measure of
reactive stream separation. The method of determining reactive stream
separation in this study was qualitative and subjective; however, the
results obtained were consistent with those of the related effort con-
ducted by Aerojet (Contract NAS9-14186).

8.0 REFERENCES

1. Elverum, G. W., Jr., and P. Staudhammer: <u>The Effect of Rapid Liquid-Phase Reactions on Injector Design and Combustion in Rocket Motors</u>, Progress Report 30-4, Jet Propulsion Laboratory, Pasadena, California, August 1959.

2. Johnson, B. H.: <u>An Experimental Investigation of the Effects of Combustion on the Mixing of Highly Reactive Liquid Propellants</u>, Technical Report 32-689, Jet Propulsion Laboratory, Pasadena, California, July 1965.

3. Stanford, H. B., and W. H. Tyler: "Injector Development", <u>Supporting Research and Advanced Development</u>, Space Programs Summary 37-51, Vol. IV, Jet Propulsion Laboratory, Pasadena, California, February 1965, p. 192.

4. Stanford, H. B.: "Injector Development," <u>Supporting Research and Advanced Development</u>, Space Programs Summary 37-36, Vol. IV, Jet Propulsion Laboratory, Pasadena, California, December 1965, p. 174.

5. Riebling, R. W.: "Injector Development: Stream Separation Experiments," <u>Supporting Research and Advanced Development</u>, Space Program Summary 37-45, Vol. IV, Jet Propulsion Laboratory, Pasadena, California, 30 June 1967.

6. Riebling, R. W.: "Injector Development: Stream Separation Experiments," <u>Supporting Research and Advanced Development</u>, Space Program Summary 37-45, Vol. IV, Jet Propulsion Laboratory, Pasadena, California, 30 June 1967.

7. Woodward, J. W.: "Combustion Effects in Sprays," <u>Supporting Research and Advanced Development</u>, Space Programs Summary 37-36, Vol. IV, Jet Propulsion Laboratory, Pasadena, California, December 1965.

8. Burrows, M. C. (NASA-Lewis Research Center): <u>Mixing and Reaction Studies of Hydrazine and Nitrogen Tetroxide Using Photographic and Spectral Techniques,</u> AIAA Paper No. 67-107, presented at the AIAA 5th Aerospace Science Meeting, New York, N. Y., January 1967.

9. Lawver, B. R., and B. P. Breen: Hypergolic Stream Impingement Phenomena - Nitrogen Tetroxide/Hydrazine, NAS-CR-72444, Dynamic Science Division, Marshall Industries, Monrovia, California, October 1968.

10. Zung, L. B. (Dynamic Science Corporation, Monrovia, California): Hypergolic Impingement Mechanisms and Criteria for Jet Mixing or Separation, presented at the 6th ICRPG Liquid Propellant Combustion Instability Conference, 9-11 September 1969.

11. R-7223: Reactive Stream Impingement, Rocketdyne, a division of Rockwell International, 29 September 1967.

12. Houseman, J. (Jet Propulsion Laboratory, Pasadena, California): Jet Separation and Optimum Mixing for an Unlike Doublet, presented at the 6th ICRPG Liquid Propellant Combustion Instability Conference, 9-11 September 1969.

13. Campbell, D. T., Photographic Study of Hypergolic Propellant Stream Blowapart, presented at AIAA Joint Specialists Conference, San Diego, California, 1970.

14. Kushida, R., and J. Houseman: Criteria for Separation of Impinging Streams of Hypergolic Propellants, JPL Report WSCI-67-38, 1967.

15. Wuerker, R. F., B. J. Matthews, and R. A. Briones (TRW Systems Group): Producing Holograms of Reacting Sprays in Liquid Propellant Rocket Engines, TRW Report 68.4712.2-024, 31 July 1968.

16. Lee, A., and J. Houseman: Popping Phenomena with N_2O_4/N_2H_4 Injectors, presented at the Western States Section Meeting of the Combustion Institute on Stable Combustion of Liquid Propellants, JPL, October 26-27, 1970.

17. Clayton, R.: Experimental Observations Relating the Inception of Liquid Rocket Engine Popping and Resonant Combustion to the Stagnation Dynamics of Injection Impingement, TR 32-1479, JPL, 15 December 1970.

18. Perlee, H., et al.: Hypergolic Ignition and Combustion Phenomena in the Propellant System Aerozine - 50/N_2O_4, Final Report No. 4019, Bureau of Mines, Pittsburgh, Pennsylvania, April 1, 1965 to March 31, 1967.

19. Friedman, R., et al.: A Study of Explosions Induced by Contact of Hydrazine-type Fuels with Nitrogen Tetroxide, Technical Document ASD-TDR-62-685, Atlantic Research Corporation, September 1962.

20. Rodriguez, S., and A. Axworthy: Liquid Phase Reactions of Hypergolic Propellants, R-8374, Rocketdyne, a division of Rockwell International, Canoga Park, California, December 1970.

21. Nurick, W., and J. Cordill: Reactive Stream Separation Photography, Final Report, R-8490, Rocketdyne, a division of Rockwell International, Canoga Park, California, May 1972.

22. Lawver, B. R.: Rocket Engine Popping Phenomena, Aerojet General Report No. TCER 9642:0095, March 1969.

23. Houseman, J.: Jet Separation and Popping with Hypergolic Propellants, presented at the 7th JANNAF Combustion Meeting, CPIA Publication 204, Vol. 1, February 1971, pp 445-453.

24. Lawver, B. R.: A Model of the Hypergolic Pop Phenomena, J. Spacecraft and Rockets, Vol. 9, No. 4, April 1972, pp 225-226.

25. Hines, W. S., and W. H. Nurick, High Performance N_2O_4/Amine Elements Task I Literature Review, Contract NAS9-14126, R-9594, Rocketdyne Division, Rockwell International, September 1974.

26. Rupe, J. H., A Correlation Between the Dynamic Properties of a Pair of Impinging Streams and the Uniformity of Mixture Ratio Distribution in the Resulting Spray, Progress Report No. 20-209, Jet Propulsion Laboratory, Pasadena, Calif., 28 March 1956.

27. Lawver, B. R., High Performance N_2O_4/Amine Elements - "Blowapart", Task III Data Dump, Contract NAS9-14186, Report 14186-DR6-3-1, Aerojet Liquid Rocket Company, 15 November 1974.

9.0 NOMENCLATURE

A   Zero order reaction rate constant (sec^{-1})

B   Critical rate coefficient (ft^{-1})

C_p Specific heat of liquid (Btu/lb ^oR)

C_1 Critical sheet length coefficient (200 ft/sec)

C_2 Critical mixing zone coefficient (2)

d   Orifice diameter

D   Mean jet diameter (ft)

ΔE Activation energy (lbf-ft/lb mole ^oR)

ΔH Heat of reaction (Btu/lb mole gas)

K_1 Lumped coefficient for integration

L_c Critical hydrodynamic length (ft)

MR   Mixture ratio ($\dot{W}_{ox}/\dot{W}_f$)

P   Pressure in fan (lbf/ft^2)

P_c Chamber pressure (lbf/ft^2)

Q   Volumetric heat generation (Btu/ft^3)

$\mathcal{R}$ Reaction rate volume/volume-sec

R_g Gas constant (1544 lbf ft/lb mole ^oR)

T   Temperature (^oR)

t   Time (sec)

U   Fan velocity (ft)

v   Injection velocity

V	Specific volumetric gas generation (volume/volume)
$\dot{W}$	Flowrate
x	Distance along fan (ft)
ρ_g	Density of gas (lb mole/ft^3)
ρ_ℓ	Density of liquid (lb/ft^3)
ϕ	Mixing index

Subscript

c	Critical
g	Gas
ℓ	Liquid
o	At impingement point
f	Fuel
ox	Oxidizer

10.0 APPENDIX A

TABLE OF AEROJET DATA FROM CONTRACT NAS9-14186

This appendix contains a table of the experimental results of reactive stream separation experiments conducted by Aerojet Liquid Rocket Company on Contract NAS9-14186. That contract was conducted concurrently with the contract (NAS9-14126) reported herein by Rocketdyne. The results are presented here because the experiments were similar to those conducted by Rocketdyne and they were employed along with Rocketdyne's data in correlation of the experimental results. Only the test data that could be employed in correlation with the data from this contract (NAS9-14126) are included in the table.

TABLE A-1. AEROJET BLOWAPART DATA FROM CONTRACT NAS9-14286

Test No. (1)	Fuel (2)	Chamber Pressure		MR	Injection Velocity				Propellant Temperature				Result (3)
		$N/m^2 \times 10^{-6}$	psia		Oxidizer		Fuel		Oxidizer		Fuel		
					m/s	ft/sec	m/s	ft/sec	°K	°F	°K	°F	
101	MMH	2.123	308	1.66	32.9	108	39.3	129	304	88	304	87	S
102		2.123	308	1.57	32.0	105	40.2	132	304	88	304	87	S
103		2.130	309	1.62	32.3	106	39.6	130	304	88	304	87	S
104		2.144	311	1.62	32.0	105	39.3	129	304	88	304	87	S
105		3.495	507	1.70	32.9	108	38.4	126	305	89	304	88	S
106		6.894	1000	1.57	33.5	110	42.1	137	305	89	304	88	S
107		2.123	308	1.70	32.6	107	38.1	125	303	86	302	85	S
108		1.813	263	1.65	31.4	103	38.1	125	302	84	302	84	S
109		1.358	197	1.64	34.4	113	41.4	136	302	84	302	84	S
110		1.089	158	1.60	32.0	105	39.6	130	301	83	301	83	S
111		0.689	100	1.60	33.5	110	41.4	136	302	84	301	83	M
124		6.584	955	1.61	25.3	83	31.1	102	301	82	301	82	S
125		3.412	495	1.60	32.3	106	39.6	130	301	83	300	81	S
126		2.054	298	1.59	32.3	106	40.2	132	301	83	301	82	S
127		1.951	283	1.58	19.5	64	24.4	80	302	84	300	81	S
128		1.765	256	1.58	30.8	101	38.4	126	302	85	301	83	S
129	↓	1.317	191	1.60	33.2	109	41.4	136	302	85	301	83	S

(1) The injector employed was similar to Rocketdyne's UD-1 single element injector.
(2) The oxidizer for all tests was N_2O_4.
(3) S = separated; M = mixed; P = penetrated; Undef. = undefined.

TABLE A-1. (Continued)

Test No. (1)	Fuel (2)	Chamber Pressure N/m²×10⁻⁶	Chamber Pressure psia	MR	Injection Velocity Oxidizer m/s	Oxidizer ft/sec	Fuel m/s	Fuel ft/sec	Propellant Temperature Oxidizer °K	Oxidizer °F	Fuel °K	Fuel °F	Result (3)
130	MMH	1.048	152	1.56	31.1	102	39.6	130	302	85	301	82	S
131		0.655	95	1.57	32.3	106	40.5	133	302	85	301	83	M
132		0.786	114	1.58	33.2	109	41.4	136	303	86	301	83	M
133		2.833	411	1.66	45.7	150	54.9	180	301	83	301	83	S
134		0.669	97	1.74	33.5	110	41.4	136	298	77	365	197	S
135		0.820	119	1.72	34.1	112	42.3	139	299	78	366	199	S
136		1.034	150	1.74	33.5	110	41.4	136	298	77	366	199	S
137		1.296	188	1.74	35.4	116	43.9	144	297	76	366	199	S
138		1.675	243	1.60	33.8	111	45.4	149	299	79	364	195	S
139		0.710	103	1.45	13.1	43	17.7	58	290	61	288	59	Undef.
140		0.558	81	1.61	35.4	116	43.6	148	291	64	290	62	Undef.
141		0.558	81	1.60	35.0	115	43.6	143	292	66	291	64	Undef.
142		0.820	119	1.59	33.2	109	41.8	137	293	68	292	67	M
143		0.889	129	1.42	11.9	39	16.4	54	292	67	292	67	Undef.
144		1.062	154	1.53	13.1	43	17.1	56	292	67	292	67	Undef.
145		1.048	152	1.62	32.0	105	39.0	128	293	68	292	67	S
146		1.310	190	1.57	32.9	108	41.4	136	293	68	292	67	S
147		1.779	258	1.61	30.8	101	37.8	124	293	68	292	67	S
148		0.703	102	1.49	13.4	44	18.0	59	293	68	293	68	M

(1) The injector employed was similar to Rocketdyne's UD-1 single Element injector.
(2) The oxidizer for all tests was N_2O_4.
(3) S = separated; M = mixed; P = penetrated; Undef. = undefined.

TABLE A-1. (Continued)

Test No. (1)	Fuel (2)	Chamber Pressure		MR	Injection Velocity				Propellant Temperature				Result (3)
		N/m²×10⁻⁶	psia		Oxidizer		Fuel		Oxidizer		Fuel		
		$N/m^2 \times 10^{-6}$	psia		m/s	ft/sec	m/s	ft/sec	°K	°F	°K	°F	
149	MMH	0.682	99	1.60	32.6	107	40.8	134	294	69	294	69	M
150		2.048	297	1.62	32.6	107	40.2	132	294	70	294	69	S
151		3.337	484	1.64	34.7	114	42.1	138	294	70	294	69	S
152		6.604	958	1.62	36.9	121	45.1	148	299	78	296	74	S
153		0.676	98	1.38	8.8	29	15.2	50	286	55	286	56	P
154		0.689	100	1.68	8.8	29	12.8	42	285	54	286	55	P
155		0.703	102	1.72	11.3	37	15.5	51	285	54	285	54	P
156		0.738	107	1.53	14.9	49	23.5	77	285	53	285	54	M
157		0.703	102	1.62	16.2	53	24.1	79	285	53	285	54	M
158		0.696	101	1.94	8.5	28	10.4	34	287	58	287	58	P
159		0.682	99	1.69	9.1	30	13.1	43	287	57	287	58	P
160		0.692	101	1.66	11.9	39	17.1	56	287	57	287	58	P
161		0.703	102	1.55	11.6	38	17.7	58	287	58	287	58	P
162		0.703	102	1.83	12.5	41	16.4	54	287	57	287	58	P
163		0.676	98	1.65	17.7	58	25.9	85	287	58	287	58	M
164		0.689	100	1.66	15.2	50	21.9	72	286	56	287	57	M
165		0.655	95	1.62	21.9	72	32.6	107	286	56	287	57	M
166		0.655	95	1.64	28.0	92	40.8	134	286	56	287	57	M

(1) The injector employed was similar to Rocketdyne's UD-1 single element injector.
(2) The oxidizer for all tests was N_2O_4.
(3) S = separated; M = mixed; P = penetrated; Undef. = undefined.

TABLE A-1. (Continued)

Test No. (1)	Fuel (2)	Chamber Pressure		MR	Injection Velocity				Propellant Temperature				Result (3)
		$N/m^2 \times 10^{-6}$	psia		Oxidizer		Fuel		Oxidizer		Fuel		
					m/s	ft/sec	m/s	ft/sec	°K	°F	°K	°F	
167	MMH	0.682	99	1.65	15.2	50	22.6	74	286	55	286	55	M
168		0.682	99	1.65	15.5	51	22.6	74	286	55	286	55	M
169		0.655	95	1.68	-	-	-	-	280	44	280	44	Undef.
170		0.614	89	1.64	-	-	49.4	162	280	44	280	44	S
171		0.655	95	1.65	33.2	109	48.8	160	280	44	280	44	S
172		1.351	196	1.87	13.4	44	17.4	57	280	44	280	44	P
173		1.365	198	1.69	13.1	43	18.9	62	280	44	280	44	M
174		1.386	201	1.64	15.8	52	23.5	77	279	43	280	44	M
175		1.324	192	1.66	21.3	70	31.1	102	279	43	280	44	M/S
176		0.669	97	1.66	15.5	51	22.9	75	283	50	283	50	M
177		0.669	97	1.68	15.5	51	22.6	74	282	48	282	49	M
178		0.662	96	1.66	14.9	49	21.6	71	281	47	282	48	M
179		0.669	97	1.67	15.8	52	22.9	75	291	64	293	58	M
180		1.392	202	1.70	15.2	50	21.3	70	292	66	295	71	M
181		2.034	295	1.60	15.2	50	22.9	75	292	67	296	73	M
182		1.255	182	1.62	33.2	109	48.8	160	297	75	298	78	S
183		1.365	198	1.62	31.4	103	46.0	151	297	76	298	77	S
184		1.786	259	1.57	21.9	72	33.2	109	295	71	294	70	S
185		1.854	269	1.64	21.0	69	30.5	100	294	70	294	70	Undef.

(1) The injector employed was similar to Rocketdyne's UD-1 single element injector.
(2) The oxidizer for all tests was N_2O_4.
(3) S = separated; M = mixed; P = penetrated; Undef. = undefined.

TABLE A-1. (Continued)

Test No. (1)	Fuel (2)	Chamber Pressure		MR	Injection Velocity				Propellant Temperature				Results (3)
					Oxidizer		Fuel		Oxidizer		Fuel		
		$N/m^2 \times 10^{-6}$	psia		m/s	ft/sec	m/s	ft/sec	°K	°F	°K	°F	
186	MMH	1.806	262	1.51	15.2	50	24.1	79	294	69	294	70	M
187		2.020	293	1.69	13.4	44	15.8	52	293	68	294	69	M
188		2.068	300	1.58	16.4	54	24.7	81	294	70	294	70	M/S
189		2.034	295	1.57	27.4	90	41.4	136	296	73	295	72	S
190		0.682	99	1.64	15.5	51	22.6	74	291	64	301	82	M
191		0.676	98	1.64	15.8	52	23.5	77	290	62	307	93	M
192		0.676	98	1.69	15.8	52	23.2	76	295	71	338	149	M/S
193		0.676	98	1.70	15.8	52	23.2	76	298	78	354	177	M/S
194		0.682	99	1.73	16.2	53	23.8	78	300	80	366	200	M/S
195		1.392	202	1.77	15.2	50	21.9	72	301	82	364	196	S
196		1.392	202	1.69	15.2	50	21.6	71	324	124	354	178	S
197		1.392	202	1.69	14.9	49	20.7	68	317	112	305	89	M
287		0.855	124	1.63	14.9	49	21.9	72	295	72	301	82	M
288		0.676	98	1.62	11.9	39	17.7	58	296	73	295	72	P
289		0.538	78	1.54	9.8	32	15.2	50	297	75	297	76	P
290		0.538	78	1.62	10.0	33	14.9	49	297	75	297	75	P
291		1.013	147	1.66	18.0	59	25.6	84	297	75	297	75	M
292		1.365	198	1.65	24.1	79	34.7	114	297	76	297	76	M/S

(1) The injector employed was similar to Rocketdyne's UD-1 single element injector.
(2) The oxidizer for all tests was N_2O_4.
(3) S = separated; M = mixed; P = penetrated; Undef. = undefined.

TABLE A-1. (Concluded)

Test No. (1)	Fuel (2)	Chamber Pressure		MR	Injection Velocity				Propellant Temperature				Results (3)
					Oxidizer		Fuel		Oxidizer		Fuel		
		$N/m^2 \times 10^{-6}$	psia		m/s	ft/sec	m/s	ft/sec	°K	°F	°K	°F	
293	MMH	0.848	123	1.68	15.5	51	23.5	77	297	75	358	185	S
294	→	0.848	123	1.74	15.5	51	23.8	78	300	80	394	249	S
295		0.834	121	1.65	16.2	53	25.3	83	320	116	388	240	S
296		1.000	145	1.71	19.5	64	30.2	99	328	131	416	290	S
297		0.993	144	1.65	20.4	67	32.0	105	340	152	418	294	S

(1) The injector employed was similar to Rocketdyne's UD-1 single element injector.
(2) The oxidizer for all tests was N2O4.
(3) S = separated; M = mixed; P = penetrated; Undef. = undefined.

11.0 APPENDIX B

ESTIMATION OF CHEMICAL REACTION NECESSARY
TO PRODUCE SEPARATION

To calculate a critical chemical reaction rate, one first estimates the density ratio (ρ_g/ρ_L) in the spray fan mixing zone. If this ratio is large, the percent reaction required to violently expand the fan (blowapart) is small. By the ideal gas law

$$\rho_g = \frac{\overline{MW}}{359}\left(\frac{P}{14.7}\right)\left(\frac{460}{T}\right) \tag{B-1}$$

From Equation (6-2)

$$\overline{MW} = \frac{2(28) + 3(18) + 28}{2 + 3 + 1} = 23$$

For applications similar to the OME thrust chamber, a pressure of 10 atm (147 psia) provides an appropriate example. Although the gas temperature is difficult to define, the proposed theoretical model assumes it to be in equilibrium with the surrounding liquid. A temperature of 600°R can therefore be assigned. Then, from Equation (B-1),

$$\rho_g = \left(\frac{23}{359}\right)\left(\frac{14.7}{14.7}\right)\left(\frac{460}{600}\right) = .489 \text{ lb/ft}^3$$

For a mixture ratio (MR) of 1.6, the liquid density is given by

$$\rho_L = \frac{1 + MR}{\dfrac{1}{\rho_{MMH}} + \dfrac{MR}{\rho_{N_2O_4}}} = \frac{1 + 1.6}{\dfrac{1}{55} + \dfrac{1.6}{90}} \approx 72 \text{ lb/ft}^3$$

$$\rho_g/\rho_L = \frac{.489}{72} = .0067$$

If only .0067 (approximately 1/2 percent) of the liquid propellants react in the liquid sheet, the gas formed will occupy the same volume as the total reacting liquids. A blowapart condition therefore requires only a very small fraction of the liquid propellants to react.

C-2

12.0 APPENDIX C

DISTRIBUTION LIST

One (1) microfiche and fifty (50) copies as follows:

NASA/Lyndon B. Johnson Space Center
Primary Propulsion Branch
Attn: M. F. Lausten, Mail Code EP2
Houston, TX 77058
(1 microfiche & 1 copy - ADDRESSEE)

NASA/Lyndon B. Johnson Space Center
R&T Procurement Branch
Attn: Tommy McPhillips, Mail Code BC72 (4)
Houston, TX 77058
(1 copy)

NASA/Lyndon B. Johnson Space Center
Technical Library Branch
Attn: Retha Shirkey, Mail Code JM6
Houston, TX 77058
(4 copies)

NASA/Lyndon B. Johnson Space Center
Management Services Division
Attn: John T. Wheeler, Mail Code AT3
Houston, TX 77058
(1 copy)

NASA/Lyndon B. Johnson Space Center
Houston, Texas 77058
Attn: Distribution Operations Section/JM86
        (43 copies)